第 41 卷第 4 期
2024 年 4 月

控 制 理 论 与 应 用
Control Theory & Applications

Vol. 41 No. 4
Apr. 2024

存在未知时滞非线性系统的迭代变区间预测迭代学习控制

余琼霞[1†], 田丰臣[1], 孙俊杰[2], 侯忠生[3]

(1. 河南理工大学 电气工程与自动化学院, 河南 焦作 454000; 2. 焦作煤业(集团)有限责任公司铁路运输处, 河南 焦作 454000;
3. 青岛大学 自动化学院, 山东 青岛 266071)

摘要: 本文针对机理模型未知的非线性非仿射多入多出(MIMO)离散时间系统, 研究了系统同时存在未知时滞和迭代变化运行时间区间的预测迭代学习控制(PILC)问题. 首先利用未知时滞的上下界信息建立了一种新型的动态线性化(DL)模型, 理论分析表明该模型能够等价描述本文所考虑的存在未知时滞的未知非线性系统. 同时, 设计一种新的数据补偿机制用以处理由于系统运行时间区间迭代变化而引起的数据丢失问题. 基于所建立的DL模型和数据补偿机制, 设计了能够同时处理未知时滞和迭代变化运行时间区间的预测迭代学习控制方法. 通过严格的理论分析同时给出了建模误差和跟踪控制误差的收敛性质. 最后, 通过仿真进一步验证了所提方法的有效性.

关键词: 迭代学习控制; 预测迭代学习控制; 未知时滞; 迭代变区间

引用格式: 余琼霞, 田丰臣, 孙俊杰, 等. 存在未知时滞非线性系统的迭代变区间预测迭代学习控制. 控制理论与应用, 2024, 41(4): 701 – 715

DOI: 10.7641/CTA.2023.20521

Predictive iterative learning control for nonlinear systems with unknown time delay and iteratively varying trial lengths

YU Qiong-xia[1†], TIAN Feng-chen[1], SUN Jun-jie[2], HOU Zhong-sheng[3]

(1. School of Electrical Engineering and Automation, Henan Polytechnic University, Jiaozuo Henan 454000, China;
2. Railway Transportation Division of Jiaozuo Coal Industry (Group) Co., Ltd, Jiaozuo Henan 454000, China;
3. School of Automation, Qingdao University, Qingdao Shandong 266071, China)

Abstract: This paper investigates the predictive iterative learning control (PILC) problem for a class of nonlinear and nonaffine multiple-input multiple-output (MIMO) discrete-time systems with unknown system mechanism model and under both unknown time delay and iteratively varying trial lengths. First, a new dynamic linearization (DL) model is developed by virtue of the upper and lower bound information of the unknown time delay, and the theoretical analysis shows that the constructed model can equivalently describe the unknown nonlinear system with unknown time delay considered in this paper. At the same time, a new data compensation mechanism is introduced to deal with the problem of data loss caused by the varying trial lengths at each iteration of the system. Based on the developed DL model and data compensation mechanism, a predictive iterative learning control method is designed that can handle both the unknown time delay and the iteratively varying trial lengths. The convergence properties of both the modeling error and the tracking control error are given through rigorous theoretical analysis. Simulation results further verify the effectiveness of the proposed method.

Key words: iterative learning control; predictive iterative learning control; unknown time delay; iteratively varying trial lengths

Citation: YU Qiongxia, TIAN Fengchen, SUN Junjie, et al. Predictive iterative learning control for nonlinear systems with unknown time delay and iteratively varying trial lengths. *Control Theory & Applications*, 2024, 41(4): 701 – 715

收稿日期: 2022−06−13; 录用日期: 2023−05−10.

†通信作者. E-mail: qiongxiayu@hotmail.com; Tel.: +86 18839179003.

本文责任编委: 侯增广.

国家自然科学基金项目(62003133, 61833001), 河南省自然科学基金项目(202300410177), 河南省高校基本科研业务费专项资金项目(NSFRF200324, NSFRF210449), 河南省高等学校重点科研项目(20B413002), 河南理工大学杰出青年基金项目(J2023–5)资助.

Supported by the National Natural Science Foundation of China (62003133,61833001), the National Natural Science Foundation of Henan Province (202300410177), the Fundamental Research Funds for the Universities of Henan Province (NSFRF200324, NSFRF210449), the Key Scientific Research Projects of Universities in Henan Province (20B413002) and the Outstanding Youth Science Foundation of Henan Polytechnic University (J2023–5).

1 引言

迭代学习控制(iterative learning control, ILC)针对具有重复性运行特性的系统, 根据系统历史的输入与输出信息, 不断地调节控制信号, 进而使系统实际输出能够在有限的时间间隔内实现对期望输出的完全跟踪. ILC由日本学者M.Uchiyama首次提出, 随后Arimoto在1984年研究机器人使用该方法[1], 推动了ILC的发展, 随后ILC便成为控制领域的热点问题, 引起了学者们的广泛关注. 目前为止, ILC已广泛应用于实际工业领域, 如高速列车[2–4]、电机[5–6]、机器人[7–9]、智能电源开关[10]等.

对于实际复杂的工业过程, 模型预测控制(model predictive control, MPC)[11]得到了广泛的研究. 该方法能够提供在复杂情况下利用过程信息实现优化控制的途径, 根据实际系统的特点和控制要求建立预测模型, 通过某种性能指标最优来确定未来的控制作用, 从而实现较高的控制品质和经济效益.

近年来, 学者们致力于将模型预测控制与迭代学习控制有机结合, 优势互补, 旨在通过学习更多的系统信息设计出能够保证某些性能指标达到最优的控制策略[12–20]. 文献[12–15]在2维系统理论框架下设计了模型预测迭代学习控制方法. 文献[16–18]为模型已知的线性系统设计了相应的预测迭代学习控制方法. 文献[19–20]基于已知的非线性系统模型设计了预测迭代学习控制方法. 值得指出的是, 上述关于模型预测迭代学习控制的研究工作[12–20]均需依赖系统的模型信息, 而随着现代工业的高速发展, 系统装置、运行过程及运行环境日益复杂化, 单纯依靠机理分析很难确切掌握系统的动态特性, 因而无法精确建立实际系统的动力学模型. 因此, 需要设计不依赖系统模型信息的预测迭代学习控制方法. 目前, 针对未知非线性系统的预测迭代学习控制研究工作少之又少. 文献[21]针对完全未知的多输入多输出 (multiple input and multiple output, MIMO)的非线性离散系统, 设计了无约束和有约束情况下的数据驱动预测迭代学习控制 (date-driven predictive ILC, DDPILC). 文献 [22] 提出了基于径向基函数神经网络的DDPILC, 进一步考虑了未知外部扰动的影响. 但上述研究工作[21–22]存在2个局限: 1) 要求系统每次运行的时间区间固定不变; 2) 没有考虑时滞对系统的影响.

实际上, ILC方法的基本假设之一是要求系统在固定并且严格重复的时间区间内进行重复运动. 然而在实际工程中, 系统每次重复运行的时间区间经常是迭代变化的. 例如, 高速列车每天应该按照运行图在固定的时间区间内重复执行相同的旅客运输任务, 但实际上列车经常会出现早到或晚点的情况, 从而导致实际的运行时间区间迭代变化. 在ILC领域, 文献[23]针对迭代变区间的线性离散系统, 设计了反馈辅助比例微分(proportional-derivative, PD)型量化迭代学习控制算法. 文献[24]针对非线性多智能体系统, 研究了分布式变区间无模型自适应迭代学习控制的一致性跟踪问题. 文献[25]针对模型结构已知的线性系统, 设计了相应的变区间迭代学习控制方法. 文献[26]针对离散时间仿射非线性系统, 提出了一种能够保证严格点态收敛的变区间迭代学习控制方法. 文献[27]针对多入多出的离散仿射非线性系统, 设计了高阶的迭代学习控制算法. 上述研究工作[23–27]中, 当前批次控制输入的更新如果用到前一次迭代未运行时刻的数据, 将该时刻缺失的输出误差数据进行补零. 将误差数据直接补零将导致无法对控制输入进行有效更新. 因此, 如何利用历史实际运行数据信息及历史运行过程中对未来运行时刻的预报信息对缺失运行时刻的数据进行更加有效的补偿, 并设计相应的预测迭代学习控制方法, 目前还没有相关研究工作.

另一方面, 时滞现象广泛存在于实际受控系统中. 文献[28]针对含有已知时不变的输入时滞线性系统建立一种嵌套预测反馈方法对输入时滞进行补偿. 文献[29]针对含有未知时变时滞的线性系统, 假设当前时刻时滞已知, 提出了一种基于预测的可变输入时滞控制方法. 针对模型结构已知的仿射非线性系统, 文献[30]针对已知的时不变输入时滞设计了一种状态反馈镇定控制器, 文献[31]通过使用泰勒定理对含有已知时变时滞的输入进行近似, 提出了一种基于高增益观测器的时滞重构方法. 然而, 如何针对含有未知时变时滞且系统模型未知的非线性非仿射系统设计相应的预测迭代控制方法, 具有一定的挑战性.

鉴于以上分析, 本文首次同时考虑未知时变的输入时滞和迭代变化的运行时间区间, 借助未知时滞的上下界信息, 并设计一种新型的缺失数据补偿机制, 为未知的非线性非仿射系统设计了不依赖系统机理模型信息的预测迭代学习控制方法, 并同时给出了所提出方法的收敛性质. 系统整体结构框图如图1所示.

2 问题表述

考虑含有未知时滞的可重复的多入多出非线性非仿射离散时间系统

$$\begin{aligned}&\boldsymbol{y}_k(t+1)=\\&\boldsymbol{f}(\boldsymbol{y}_k(t),\boldsymbol{y}_k(t-1),\cdots,\boldsymbol{y}_k(t-n_y),\\&\boldsymbol{u}_k(t-h(t)),\boldsymbol{u}_k(t-h(t)-1),\cdots,\\&\boldsymbol{u}_k(t-h(t)-n_u)),\end{aligned}\tag{1}$$

其中: 下标$k\in\mathbb{N}^+$表示迭代次数, $t\in\{0,1,\cdots,T_k\}$表示运行时间; T_k是系统第k次运行的实际运行长度; $h(t)\in\mathbb{R}$是未知且时变的输入时滞, 且$\tau_1(t)\leqslant h(t)\leqslant\tau_2(t)$; $\tau_2(t),\tau_1(t)$是时变但已知的时滞上下界; $\boldsymbol{y}_k(t)$

$\in \mathbb{R}^n$和$\boldsymbol{u}_k(t) \in \mathbb{R}^n$是系统在第$k$次迭代$t$时刻的输出和输入, $n_u \in \mathbb{N}^+$和$n_y \in \mathbb{N}^+$是未知的系统阶数; $\boldsymbol{f}(\cdot) \in \mathbb{R}^n$是未知的非线性函数.

记T_d为期望的固定运行时间长度, 系统的实际跟踪控制误差$\boldsymbol{e}_k(t+1)$定义为

$$\begin{aligned}&\boldsymbol{e}_k(t+1) = \boldsymbol{y}_d(t+1) - \boldsymbol{y}_k(t+1),\\&0 \leqslant t \leqslant \min\{T_k, T_d\},\end{aligned} \tag{2}$$

其中$\boldsymbol{y}_d(t+1), t \in \{0,1,\cdots,T_d\}$是期望的系统输出.

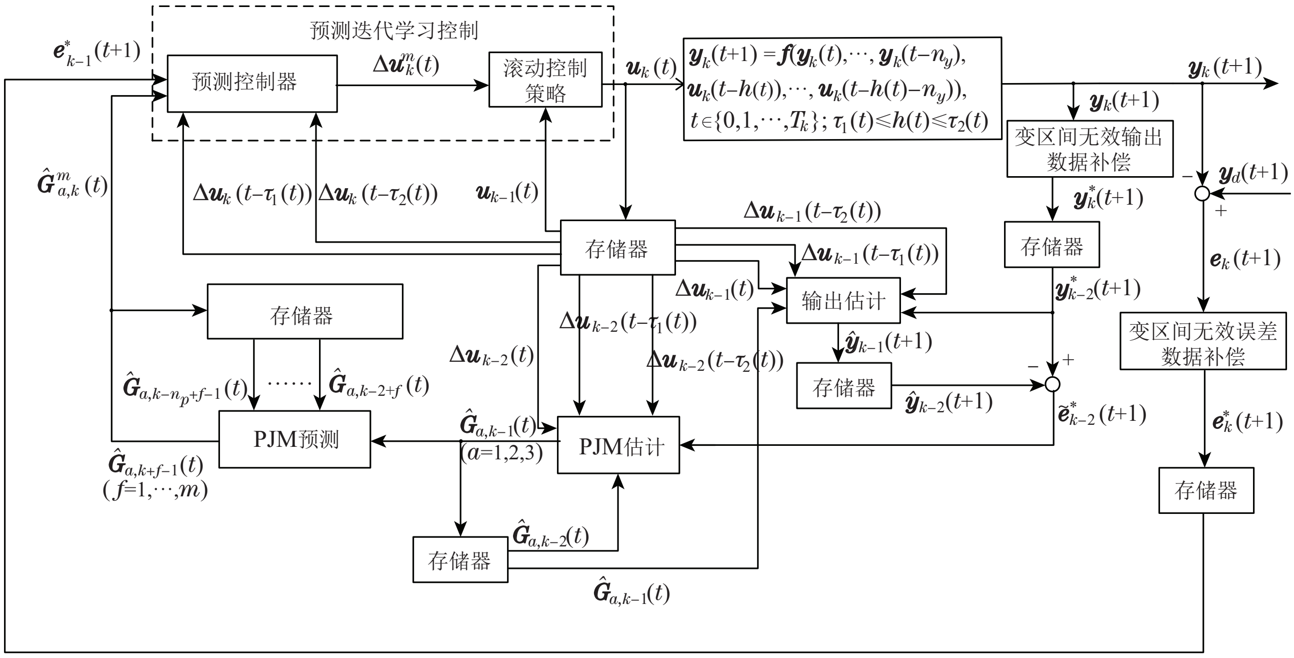

图 1　系统结构框图

Fig. 1　System structure block diagram

为了有效处理迭代变化的运行时间长度问题, 实现整个期望运行时间区间$t \in \{0,1,\cdots,T_d\}$上的跟踪控制, 引入如下新的跟踪控制误差:

$$\boldsymbol{e}^*_k(t+1) = \begin{cases} \varrho_k(t+1)\boldsymbol{e}_k(t+1) + \\ \{\sum\limits_{i=1}^{2}[\prod\limits_{j=1}^{i}(1-\varrho_{k-j+1}(t+1))]\cdot \\ \varrho_{k-i}(t+1)\boldsymbol{e}_{k-i}(t+1) + \\ [\prod\limits_{j=1}^{3}(1-\varrho_{k-j+1}(t+1))]\cdot \\ \boldsymbol{e}^*_{k|k-1}(t+1)\},\ T_k \leqslant T_d, \\ \boldsymbol{e}_k(t+1), \qquad T_k \geqslant T_d, \end{cases} \tag{3}$$

其中: $\varrho_k(t+1)$是一个判断函数, 只取0和1, 当系统在第k次迭代的$t+1$时刻存在真实的误差值$\boldsymbol{e}_k(t+1)$, 则$\varrho_k(t+1)=1$, 式(3)可被写为$\boldsymbol{e}^*_k(t+1) = \boldsymbol{e}_k(t+1)$; 当系统在第$k$次迭代的$t+1$时刻没有真实的误差值$\boldsymbol{e}_k(t+1)$存在时, 则$\varrho_k(t+1) = 0$, 此时搜索历史$k-1$次运行该时刻的值. 若可搜索到真实的误差值$\boldsymbol{e}_{k-1}(t+1)$, 则$\varrho_{k-1}(t+1) = 1$, 式(3)可被写为$\boldsymbol{e}^*_k(t+1) = \boldsymbol{e}_{k-1}(t+1)$. 若没有搜到真实的误差值, 则继续搜索历史$k-2$次运行该时刻的值. 如果能够搜到真实的误差值$\boldsymbol{e}_{k-2}(t+1)$, 则$\varrho_{k-2}(t+1) = 1$, 式(3)可被写为$\boldsymbol{e}^*_k(t+1) = \boldsymbol{e}_{k-2}(t+1)$. 为了避免使用太过久远的历史数据信息进行数据补偿, 如果历史$k-1$和$k-2$次运行该时刻均搜索不到实际的误差值, 则停止搜索, 利用预报的误差值进行补偿, 式(3)可被写为$\boldsymbol{e}^*_k(t+1) = \boldsymbol{e}^*_{k|k-1}(t+1)$, 其中$\boldsymbol{e}^*_{k|k-1}(t+1)$表示在第$k-1$次迭代时预测未来第$k$次迭代的跟踪控制误差, 将在式(15)中详细介绍.

假设 1　$\forall k \in \mathbb{N}^+$, 系统的初始输出$\boldsymbol{y}_k(0)$可随机变化但需有界.

假设 2　$\forall t \in \{0,1,\cdots,T_d\}$和$k = 0,1,2\cdots$, $\boldsymbol{f}(\cdot)$关于$\boldsymbol{u}_k(t)$的偏导数存在且连续.

假设 3　系统满足广义Lipschitz条件, 即$\forall t \in \{0,1,\cdots,T_d\}$和$k = 0,1,2\cdots$有

$$\|\boldsymbol{y}_{k_1}(t+1) - \boldsymbol{y}_{k_2}(t+1)\| \leqslant b\|\boldsymbol{u}_{k_1}(t) - \boldsymbol{u}_{k_2}(t)\|,$$

其中: $\boldsymbol{u}_{k_1}(t) \neq \boldsymbol{u}_{k_2}(t)$; 对于任意的$k_1 \neq k_2, k_1, k_2 > 0$, $b > 0$是一个常数.

注 1　从实际角度出发, 假设2和假设3是合理且可接受的[32–33]. 假设2是控制设计中对一般非线性系统的一种典型约束条件. 假设3是对系统输出变化率上界的一种限制, 从能量的角度来看, 如果控制输入的能量变化处于一个有限的水平, 那么系统内部的能量变化不能达到无限大. 许多工业系统满足这一假设, 如压力控制系统、温度控制系统、液位控制

系统等.

定理 1 如果系统(1)满足假设1–3, 对于$t \in \{0, 1, \cdots, T_d\}$和$k = 0, 1, 2, \cdots$且$\|\Delta \boldsymbol{u}_k(t)\| \neq 0$, 则必存在伪Jacobian矩阵(pseudo Jacobian matrix, PJM) $\boldsymbol{G}_{a,k}(t) \in \mathbb{R}^{n\times n}(a = 1, 2, 3)$, 使得非线性系统(1)可等价为如下包含未知时滞上下界信息的DL模型:

$$\begin{aligned}&\Delta \boldsymbol{y}_k(t+1) =\\ &\boldsymbol{G}_{1,k}(t)\Delta \boldsymbol{u}_k(t) + \boldsymbol{G}_{2,k}(t)\Delta \boldsymbol{u}_k(t-\tau_1(t)) +\\ &\boldsymbol{G}_{3,k}(t)\Delta \boldsymbol{u}_k(t-\tau_2(t)),\end{aligned} \tag{4}$$

其中:

$$\begin{aligned}&\Delta \boldsymbol{y}_k(t+1) = \boldsymbol{y}_k(t+1) - \boldsymbol{y}_{k-1}(t+1),\\ &\Delta \boldsymbol{u}_k(t) = \boldsymbol{u}_k(t) - \boldsymbol{u}_{k-1}(t),\end{aligned}$$

$$\boldsymbol{G}_{a,k}(t) = \begin{bmatrix} g_{a,11,k}(t) & g_{a,12,k}(t) & \cdots & g_{a,1n,k}(t)\\ g_{a,21,k}(t) & g_{a,22,k}(t) & \cdots & g_{a,2n,k}(t)\\ \vdots & \vdots & & \vdots\\ g_{a,n1,k}(t) & g_{a,n2,k}(t) & \cdots & g_{a,nn,k}(t)\end{bmatrix}$$

为未知但有界的伪Jacobian矩阵.

证 由系统(1)可得

$$\begin{aligned}&\Delta \boldsymbol{y}_k(t+1) =\\ &\boldsymbol{f}(\boldsymbol{y}_k(t), \boldsymbol{y}_k(t-1), \cdots, \boldsymbol{y}_k(t-n_y),\\ &\boldsymbol{u}_k(t-\tau_1(t)), \cdots, \boldsymbol{u}_k(t-h(t)), \boldsymbol{u}_k(t-1-h(t)), \cdots,\\ &\boldsymbol{u}_k(t-\tau_2(t)), \cdots, \boldsymbol{u}_k(t-n_u-h(t))) -\\ &\boldsymbol{f}(\boldsymbol{y}_{k-1}(t), \boldsymbol{y}_{k-1}(t-1), \cdots, \boldsymbol{y}_{k-1}(t-n_y),\\ &\boldsymbol{u}_{k-1}(t-\tau_1(t)), \cdots, \boldsymbol{u}_{k-1}(t-h(t)),\\ &\boldsymbol{u}_{k-1}(t-1-h(t)), \cdots, \boldsymbol{u}_{k-1}(t-\tau_2(t)), \cdots,\\ &\boldsymbol{u}_{k-1}(t-n_u-h(t))) =\\ &\boldsymbol{f}(\boldsymbol{y}_k(t), \cdots, \boldsymbol{y}_k(t-n_y), \boldsymbol{u}_k(t), \boldsymbol{u}_k(t-h(t)),\\ &\boldsymbol{u}_k(t-1-h(t)), \cdots, \boldsymbol{u}_k(t-n_u-h(t))) -\\ &\boldsymbol{f}(\boldsymbol{y}_k(t), \cdots, \boldsymbol{y}_k(t-n_y), \boldsymbol{u}_{k-1}(t), \boldsymbol{u}_k(t-h(t)),\\ &\boldsymbol{u}_k(t-1-h(t)), \cdots, \boldsymbol{u}_k(t-n_u-h(t))) +\\ &\boldsymbol{f}(\boldsymbol{y}_k(t), \cdots, \boldsymbol{y}_k(t-n_y), \boldsymbol{u}_k(t-\tau_1(t)), \cdots,\\ &\boldsymbol{u}_k(t-h(t)), \boldsymbol{u}_k(t-1-h(t)), \cdots,\\ &\boldsymbol{u}_k(t-n_u-h(t))) - \boldsymbol{f}(\boldsymbol{y}_k(t), \cdots, \boldsymbol{y}_k(t-n_y),\\ &\boldsymbol{u}_{k-1}(t-\tau_1(t)), \cdots, \boldsymbol{u}_k(t-h(t)),\\ &\boldsymbol{u}_k(t-1-h(t)), \cdots, \boldsymbol{u}_k(t-n_u-h(t))) +\\ &\boldsymbol{f}(\boldsymbol{y}_k(t), \cdots, \boldsymbol{y}_k(t-n_y), \boldsymbol{u}_k(t-h(t)),\\ &\boldsymbol{u}_k(t-1-h(t)), \cdots, \boldsymbol{u}_k(t-\tau_2(t)), \cdots,\\ &\boldsymbol{u}_k(t-n_u-h(t))) - \boldsymbol{f}(\boldsymbol{y}_k(t), \cdots, \boldsymbol{y}_k(t-n_y),\\ &\boldsymbol{u}_k(t-h(t)), \boldsymbol{u}_k(t-1-h(t)), \cdots,\\ &\boldsymbol{u}_{k-1}(t-\tau_2(t)), \cdots, \boldsymbol{u}_k(t-n_u-h(t))) +\\ &\boldsymbol{\zeta}_{1,k}(t) + \boldsymbol{\zeta}_{2,k}(t-\tau_1(t)) + \boldsymbol{\zeta}_{3,k}(t-\tau_2(t)),\end{aligned} \tag{5}$$

其中:

$$\begin{aligned}&\boldsymbol{\zeta}_{1,k}(t) =\\ &\boldsymbol{f}(\boldsymbol{y}_k(t), \cdots, \boldsymbol{y}_k(t-n_y), \boldsymbol{u}_{k-1}(t), \boldsymbol{u}_k(t-h(t)),\\ &\boldsymbol{u}_k(t-1-h(t)), \cdots, \boldsymbol{u}_k(t-n_u-h(t))) -\\ &\boldsymbol{f}(\boldsymbol{y}_k(t), \cdots, \boldsymbol{y}_k(t-n_y), \boldsymbol{u}_k(t), \boldsymbol{u}_k(t-h(t)),\\ &\boldsymbol{u}_k(t-1-h(t)), \cdots, \boldsymbol{u}_k(t-n_u-h(t))),\\ &\boldsymbol{\zeta}_{2,k}(t-\tau_1(t)) =\\ &\boldsymbol{f}(\boldsymbol{y}_k(t), \cdots, \boldsymbol{y}_k(t-n_y), \boldsymbol{u}_{k-1}(t-\tau_1(t)),\\ &\boldsymbol{u}_k(t-h(t)), \boldsymbol{u}_k(t-1-h(t)), \cdots,\\ &\boldsymbol{u}_k(t-n_u-h(t))) - \boldsymbol{f}(\boldsymbol{y}_k(t), \cdots,\\ &\boldsymbol{y}_k(t-n_y), \boldsymbol{u}_k(t-\tau_1(t)), \boldsymbol{u}_k(t-h(t)),\\ &\boldsymbol{u}_k(t-1-h(t)), \cdots, \boldsymbol{u}_k(t-n_u-h(t))),\\ &\boldsymbol{\zeta}_{3,k}(t-\tau_2(t)) =\\ &\boldsymbol{f}(\boldsymbol{y}_k(t), \cdots, \boldsymbol{y}_k(t-n_y), \boldsymbol{u}_k(t-h(t)),\\ &\boldsymbol{u}_k(t-1-h(t)), \cdots, \boldsymbol{u}_{k-1}(t-\tau_2(t)), \cdots,\\ &\boldsymbol{u}_k(t-n_u-h(t))) - \boldsymbol{f}(\boldsymbol{y}_k(t), \cdots, \boldsymbol{y}_k(t-n_y),\\ &\boldsymbol{u}_k(t-h(t)), \boldsymbol{u}_k(t-1-h(t)), \cdots,\\ &\boldsymbol{u}_k(t-\tau_2(t)), \cdots, \boldsymbol{u}_k(t-n_u-h(t))) +\\ &\boldsymbol{f}(\boldsymbol{y}_k(t), \boldsymbol{y}_k(t-1), \cdots, \boldsymbol{y}_k(t-n_y),\\ &\boldsymbol{u}_k(t-h(t)), \cdots, \boldsymbol{u}_k(t-n_u-h(t))) -\\ &\boldsymbol{f}(\boldsymbol{y}_{k-1}(t), \boldsymbol{y}_{k-1}(t-1), \cdots, \boldsymbol{y}_{k-1}(t-n_y),\\ &\boldsymbol{u}_{k-1}(t-h(t)), \cdots, \boldsymbol{u}_{k-1}(t-n_u-h(t))).\end{aligned}$$

则利用假设2可将式(5)写为

$$\begin{aligned}&\Delta \boldsymbol{y}_k(t+1) =\\ &\frac{\partial \boldsymbol{f}^*}{\partial \boldsymbol{u}_k(t)}\Delta \boldsymbol{u}_k(t) + \frac{\partial \boldsymbol{f}^*}{\partial \boldsymbol{u}_k(t-\tau_1(t))}\Delta \boldsymbol{u}_k(t-\tau_1(t)) +\\ &\frac{\partial \boldsymbol{f}^*}{\partial \boldsymbol{u}_k(t-\tau_2(t))}\Delta \boldsymbol{u}_k(t-\tau_2(t)) + \boldsymbol{\zeta}_{1,k}(t) +\\ &\boldsymbol{\zeta}_{2,k}(t-\tau_1(t)) + \boldsymbol{\zeta}_{3,k}(t-\tau_2(t)),\end{aligned} \tag{6}$$

其中:

$$\frac{\partial \boldsymbol{f}^*}{\partial \boldsymbol{u}_k(t)} = \begin{bmatrix} \frac{\partial f_1^*}{\partial u_{1,k}(t)} & \frac{\partial f_1^*}{\partial u_{2,k}(t)} & \cdots & \frac{\partial f_1^*}{\partial u_{n,k}(t)}\\ \frac{\partial f_2^*}{\partial u_{1,k}(t)} & \frac{\partial f_2^*}{\partial u_{2,k}(t)} & \cdots & \frac{\partial f_2^*}{\partial u_{n,k}(t)}\\ \vdots & \vdots & & \vdots\\ \frac{\partial f_n^*}{\partial u_{1,k}(t)} & \frac{\partial f_n^*}{\partial u_{2,k}(t)} & \cdots & \frac{\partial f_n^*}{\partial u_{n,k}(t)}\end{bmatrix},$$

$$\frac{\partial \boldsymbol{f}^*}{\partial \boldsymbol{u}_k(t-\tau_\hbar(t))}=\begin{bmatrix}\frac{\partial f_1^*}{\partial u_{1,k}(t-\tau_\hbar(t))} & \frac{\partial f_1^*}{\partial u_{2,k}(t-\tau_\hbar(t))} & \cdots & \frac{\partial f_1^*}{\partial u_{n,k}(t-\tau_\hbar(t))}\\ \frac{\partial f_2^*}{\partial u_{1,k}(t-\tau_\hbar(t))} & \frac{\partial f_2^*}{\partial u_{2,k}(t-\tau_\hbar(t))} & \cdots & \frac{\partial f_2^*}{\partial u_{n,k}(t-\tau_\hbar(t))}\\ \vdots & \vdots & & \vdots\\ \frac{\partial f_n^*}{\partial u_{1,k}(t-\tau_\hbar(t))} & \frac{\partial f_n^*}{\partial u_{2,k}(t-\tau_\hbar(t))} & \cdots & \frac{\partial f_n^*}{\partial u_{n,k}(t-\tau_\hbar(t))}\end{bmatrix},$$

$\hbar=1,2,\ \frac{\partial f_i^*}{\partial u_{j,k}(t)}(i=1,\cdots,n)(j=1,\cdots,n)$表示$f_i$关于$u_{j,k}$的偏导数在$u_{j,k-1}(t)$和$u_{j,k}(t)$之间某一点处的值.

固定k次迭代运行, 时刻t保持不变, 考虑如下含有数值矩阵$\phi_{1,k}(t)$的等式$\boldsymbol{\zeta}_{1,k}(t)=\phi_{1,k}(t)\Delta\boldsymbol{u}_k(t)$. 由于$\|\Delta\boldsymbol{u}_k(t)\|\neq 0$, 至少存在一个解$\phi_{1,k}^*(t)$使得$\boldsymbol{\zeta}_{1,k}(t)=\phi_{1,k}^*(t)\Delta\boldsymbol{u}_k(t)$. 同理可得: $\boldsymbol{\zeta}_{2,k}(t-\tau_1(t))=\phi_{2,k}(t)\Delta\boldsymbol{u}_k(t-\tau_1(t))$和$\boldsymbol{\zeta}_{3,k}(t-\tau_2(t))=\phi_{3,k}(t)\cdot\Delta\boldsymbol{u}_k(t-\tau_2(t))$分别至少存在一个解$\phi_{2,k}(t)=\phi_{2,k}^*(t)$和$\phi_{3,k}(t)=\phi_{3,k}^*(t)$使得上式成立. 令

$$\boldsymbol{G}_{1,k}(t)=\frac{\partial \boldsymbol{f}^*}{\partial \boldsymbol{u}_k(t)}+\phi_{1,k}^*(t),$$
$$\boldsymbol{G}_{2,k}(t)=\frac{\partial \boldsymbol{f}^*}{\partial \boldsymbol{u}_k(t-\tau_1(t))}+\phi_{2,k}^*(t),$$
$$\boldsymbol{G}_{3,k}(t)=\frac{\partial \boldsymbol{f}^*}{\partial \boldsymbol{u}_k(t-\tau_2(t))}+\phi_{3,k}^*(t),$$

则式(6)可写为

$$\begin{aligned}&\Delta\boldsymbol{y}_k(t+1)=\\&\boldsymbol{G}_{1,k}(t)\Delta\boldsymbol{u}_k(t)+\boldsymbol{G}_{2,k}(t)\Delta\boldsymbol{u}_k(t-\tau_1(t))+\\&\boldsymbol{G}_{3,k}(t)\Delta\boldsymbol{u}_k(t-\tau_2(t)),\end{aligned}\tag{7}$$

其中:

$$\begin{cases}\Delta\boldsymbol{y}_k(t+1)=\\ [\Delta\boldsymbol{y}_{1,k}(t+1)\ \ \cdots\ \ \Delta\boldsymbol{y}_{n,k}(t+1)]^{\rm T},\\ \boldsymbol{G}_{a,k}(t)=\left[\boldsymbol{G}_{a,1,k}^{\rm T}(t)\ \ \cdots\ \ \boldsymbol{G}_{a,n,k}^{\rm T}(t)\right]^{\rm T},\\ \boldsymbol{G}_{a,i,k}(t)=[g_{a,i1,k}(t)\ \ \cdots\ \ g_{a,in,k}(t)],\\ i=1,\cdots,n,\ a=1,2,3,\end{cases}\tag{8}$$

且由假设3可得$\boldsymbol{G}_{a,k}(t)$是有界的, 同时$\boldsymbol{G}_{a,i,k}(t)$将在定理2中被用到.　　证毕.

注 2　定理1中要求对在第k次迭代的所有时刻t都要求满足$\|\Delta\boldsymbol{u}_k(t)\|\neq 0$. 实际上, 如果在某次迭代出现$\|\Delta\boldsymbol{u}_k(t)\|=0$, 此时可以向前移动$\sigma_k\in\mathbb{N}^+$次迭代直到$\|\boldsymbol{u}_k(t)-\boldsymbol{u}_{k-\sigma_k}(t)\|\neq 0$成立后再进行线性化.

如果系统(1)满足假设1–3, 如果存在一个整数$k_0\geqslant 1$使得

$$\|\Delta\boldsymbol{u}_{k-j}(t)\|\begin{cases}=0,\ j=1,\cdots,k_0-1,\\ \neq 0,\ j=k_0,\end{cases}\tag{9}$$

那么对于任意整数$k>k_0$, 总可以找到一个有界的整数σ_k, 使得

$$\|\Delta\boldsymbol{u}_{k-j}(t)\|\begin{cases}=0,\ j=1,\cdots,\sigma_k-2,\\ \neq 0,\ j=\sigma_k-1,\end{cases}\tag{10}$$

同时一定存在一个PJM $\boldsymbol{G}_k(t)$使得系统(1)可转化为如下DL模型:

$$\begin{aligned}&\boldsymbol{y}_k(t+1)-\boldsymbol{y}_{k-\sigma_k}(t+1)=\\&\boldsymbol{G}_{1,k}(t)(\boldsymbol{u}_k(t)-\boldsymbol{u}_{k-\sigma_k}(t))+\boldsymbol{G}_{2,k}(t)(\boldsymbol{u}_k(t-\tau_1(t))-\\&\boldsymbol{u}_{k-\sigma_k}(t-\tau_1(t)))+\boldsymbol{G}_{3,k}(t)(\boldsymbol{u}_k(t-\tau_2(t))-\\&\boldsymbol{u}_{k-\sigma_k}(t-\tau_2(t))),\end{aligned}\tag{11}$$

根据数学归纳法, 与定理1的证明相类似, 可以直接得出上述结论. 由于篇幅原因, 这里省略详细的证明.

注 3　定理1中伪Jacobian矩阵(PJM)的元素反映了系统控制输入和系统输出之间的映射关系, 所针对的多入多出系统模型(1)中的不确定性, 非线性和耦合性等都被分散的融合到PJM中[34]. 而与现有的PJM投影估计算法不同[34–36], 本文将设计一种新型的PJM估计算法(具体见下述式(27)), 并将在定理2中给出本文所提PJM估计算法的理论收敛性质.

3　预测迭代学习控制方案

若不存在由变化区间引起的数据丢失问题, 则所建立的DL模型(4)可改写为

$$\begin{aligned}&\boldsymbol{y}_k(t+1)=\\&\boldsymbol{y}_{k-1}(t+1)+\boldsymbol{G}_{1,k}(t)\Delta\boldsymbol{u}_k(t)+\\&\boldsymbol{G}_{2,k}(t)\Delta\boldsymbol{u}_k(t-\tau_1(t))+\boldsymbol{G}_{3,k}(t)\Delta\boldsymbol{u}_k(t-\tau_2(t)),\end{aligned}\tag{12}$$

用$\boldsymbol{y}_d(t+1)$同时减去式(12)两边, 可得系统实际运行误差为

$$\begin{aligned}&\boldsymbol{e}_k(t+1)=\\&\boldsymbol{e}_{k-1}(t+1)-\boldsymbol{G}_{1,k}(t)\Delta\boldsymbol{u}_k(t)-\\&\boldsymbol{G}_{2,k}(t)\Delta\boldsymbol{u}_k(t-\tau_1(t))-\boldsymbol{G}_{3,k}(t)\Delta\boldsymbol{u}_k(t-\tau_2(t)).\end{aligned}\tag{13}$$

由于本文考虑变区间的问题, 未运行时间区间$(T_k,T_d]$内的数据是无效的, 且第$k-1$次迭代的时间区间$[T_{k-1},T_k]$内的数据也有可能是缺失的, 针对此类问题, 采用所提出的补偿机制式(3)进行补偿后, 可得

如下期望运行时间区间内完整且可用的误差模型:

$$\begin{aligned}&\boldsymbol{e}_k^*(t+1)=\\&\boldsymbol{e}_{k-1}^*(t+1)-\boldsymbol{G}_{1,k}(t)\Delta\boldsymbol{u}_k(t)-\\&\boldsymbol{G}_{2,k}(t)\Delta\boldsymbol{u}_k(t-\tau_1(t))-\boldsymbol{G}_{3,k}(t)\Delta\boldsymbol{u}_k(t-\tau_2(t)),\\&0\leqslant t\leqslant T_d,\end{aligned}\tag{14}$$

由式(14)可得未来$k+m$次迭代运行的跟踪误差

$$\begin{aligned}&\boldsymbol{e}_{k+m|k}^*(t+1)=\\&\boldsymbol{e}_k^*(t+1)-\sum_{f=1}^{m}[\boldsymbol{G}_{1,k+f}(t)\Delta\boldsymbol{u}_{k+f}(t)+\\&\boldsymbol{G}_{2,k+f}(t)\Delta\boldsymbol{u}_{k+f}(t-\tau_1(t))+\\&\boldsymbol{G}_{3,k+f}(t)\Delta\boldsymbol{u}_{k+f}(t-\tau_2(t))],\end{aligned}\tag{15}$$

其中$\boldsymbol{e}_{k+m|k}^*(t+1)$表示在第$k$次迭代时预测未来第$k+m$次迭代的跟踪控制误差.

分别定义PJM $\boldsymbol{G}_{a,k+1}^m(t)\in\mathbb{R}^{n\times mn}(a=1,2,3)$和$\Delta\boldsymbol{u}_{k+1}^m(t)\in\mathbb{R}^{mn\times1}$, $\Delta\boldsymbol{u}_{k+1}^m(t-\tau_1(t))\in\mathbb{R}^{mn\times1}$, $\Delta\boldsymbol{u}_{k+1}^m(t-\tau_2(t))\in\mathbb{R}^{mn\times1}$如下:

$$\boldsymbol{G}_{a,k+1}^m(t)=[\boldsymbol{G}_{a,k+1}(t)\ \ \cdots\ \ \boldsymbol{G}_{a,k+m}(t)],\tag{16}$$

$$\Delta\boldsymbol{u}_{k+1}^m(t)=[\Delta\boldsymbol{u}_{k+1}^{\mathrm{T}}(t)\ \ \cdots\ \ \Delta\boldsymbol{u}_{k+m}^{\mathrm{T}}(t)]^{\mathrm{T}},\tag{17}$$

$$\begin{aligned}&\Delta\boldsymbol{u}_{k+1}^m(t-\tau_1(t))=\\&[\Delta\boldsymbol{u}_{k+1}^{\mathrm{T}}(t-\tau_1(t))\ \cdots\ \Delta\boldsymbol{u}_{k+m}^{\mathrm{T}}(t-\tau_1(t))]^{\mathrm{T}},\end{aligned}\tag{18}$$

$$\begin{aligned}&\Delta\boldsymbol{u}_{k+1}^m(t-\tau_2(t))=\\&[\Delta\boldsymbol{u}_{k+1}^{\mathrm{T}}(t-\tau_2(t))\ \cdots\ \Delta\boldsymbol{u}_{k+m}^{\mathrm{T}}(t-\tau_2(t))]^{\mathrm{T}},\end{aligned}\tag{19}$$

则式(15)可写为

$$\begin{aligned}&\boldsymbol{e}_{k+m|k}^*(t+1)=\\&\boldsymbol{e}_k^*(t+1)-\boldsymbol{G}_{1,k+1}^m(t)\Delta\boldsymbol{u}_{k+1}^m(t)-\\&\boldsymbol{G}_{2,k+1}^m(t)\Delta\boldsymbol{u}_{k+1}^m(t-\tau_1(t))-\\&\boldsymbol{G}_{3,k+1}^m(t)\Delta\boldsymbol{u}_{k+1}^m(t-\tau_2(t)).\end{aligned}\tag{20}$$

由于式(14)中的PJM $\boldsymbol{G}_{a,k}(t)(a=1,2,3)$以及式(20)中的PJM $\boldsymbol{G}_{a,k+1}^m(t)(a=1,2,3)$是未知的, 所以需要对PJM $\boldsymbol{G}_{a,k}(t)$进行估计, 并对PJM $\boldsymbol{G}_{a,k+1}^m(t)$进行预测. 定义PJM $\boldsymbol{G}_{a,k}(t)$的估计值为$\hat{\boldsymbol{G}}_{a,k}(t)$, PJM $\boldsymbol{G}_{a,k+1}^m(t)$的预测值为$\hat{\boldsymbol{G}}_{a,k+1}^m(t)$, 且根据式(16)有

$$\hat{\boldsymbol{G}}_{a,k+1}^m(t)=[\hat{\boldsymbol{G}}_{a,k+1}(t)\ \ \cdots\ \ \hat{\boldsymbol{G}}_{a,k+m}(t)].\tag{21}$$

接下来分别对估计算法和预报算法进行设计. 定义如下建模误差:

$$\begin{aligned}&\tilde{\boldsymbol{e}}_k(t+1)=\\&\boldsymbol{y}_k(t+1)-\hat{\boldsymbol{y}}_k(t+1),\ 0\leqslant t\leqslant T_k.\end{aligned}\tag{22}$$

如果$T_k<T_d$, 则上式中实际输出$\boldsymbol{y}_k(t+1)$在未运行时间区间$(T_k,T_d]$内的数据是缺失的, 因此定义如下新的建模误差

$$\tilde{\boldsymbol{e}}_k^*(t+1)=\boldsymbol{y}_k^*(t+1)-\hat{\boldsymbol{y}}_k(t+1),\ 0\leqslant t\leqslant T_d,\tag{23}$$

$$\tilde{\boldsymbol{e}}_k^*(t+1)=[\tilde{e}_{1,k}^*(t+1)\ \cdots\ \tilde{e}_{n,k}^*(t+1)],\tag{24}$$

$\tilde{e}_{i,k}^*(t+1)(i=1,\cdots,n)$将在定理2中被用到. $\hat{\boldsymbol{y}}_k(t+1)$是实际输出$\boldsymbol{y}_k(t+1)$的估计值. 根据式(12) 可得

$$\begin{aligned}&\hat{\boldsymbol{y}}_k(t+1)=\\&\boldsymbol{y}_{k-1}^*(t+1)+\hat{\boldsymbol{G}}_{1,k}(t)\Delta\boldsymbol{u}_k(t)+\\&\hat{\boldsymbol{G}}_{2,k}(t)\Delta\boldsymbol{u}_k(t-\tau_1(t))+\hat{\boldsymbol{G}}_{3,k}(t)\Delta\boldsymbol{u}_k(t-\tau_2(t)),\end{aligned}\tag{25}$$

其中PJM $\hat{\boldsymbol{G}}_{a,k}(t)$是$\boldsymbol{G}_{a,k}(t)$的估计值$(a=1,2,3)$.

式(23)中, 实际输出$\boldsymbol{y}_k(t+1)$可能存在数据丢失的问题, 且在计算$\hat{\boldsymbol{y}}_k(t+1)$时, 式(25)也需要用到实际的输出$\boldsymbol{y}_{k-1}(t+1)$, 进而也会存在由于数据丢失无法计算的问题. 因此, 本文将直接对$\boldsymbol{y}_k(t+1)$进行补偿, 补偿后的系统输出为$\boldsymbol{y}_k^*(t+1)$, 补偿机制如下:

$$\begin{aligned}&\boldsymbol{y}_k^*(t+1)=\\&\varrho_k(t+1)\boldsymbol{y}_k(t+1)+\{\sum_{i=1}^{2}[\prod_{j=1}^{i}(1-\\&\varrho_{k-j+1}(t+1))]\varrho_{k-i}(t+1)\boldsymbol{y}_{k-i}(t+1)+\\&[\prod_{j=1}^{3}(1-\varrho_{k-j+1}(t+1))]\boldsymbol{y}_d(t+1)\},\end{aligned}\tag{26}$$

其中判断函数$\varrho_k(t+1)$的定义与式(3)中相同.

首先, 采用如下沿迭代轴的学习算法来获得PJM $\hat{\boldsymbol{G}}_{a,k}(t)(a=1,2,3)$:

$$\begin{cases}\hat{\boldsymbol{G}}_{1,k}(t)=\hat{\boldsymbol{G}}_{1,k-1}(t)+\eta_1\tilde{\boldsymbol{e}}_{k-1}^*(t+1)\Delta\boldsymbol{u}_{k-1}^{\mathrm{T}}(t),\\\hat{\boldsymbol{G}}_{2,k}(t)=\\\hat{\boldsymbol{G}}_{2,k-1}(t)+\eta_2\tilde{\boldsymbol{e}}_{k-1}^*(t+1)\Delta\boldsymbol{u}_{k-1}^{\mathrm{T}}(t-\tau_1(t)),\\\hat{\boldsymbol{G}}_{3,k}(t)=\\\hat{\boldsymbol{G}}_{3,k-1}(t)+\eta_3\tilde{\boldsymbol{e}}_{k-1}^*(t+1)\Delta\boldsymbol{u}_{k-1}^{\mathrm{T}}(t-\tau_2(t)),\end{cases}\tag{27}$$

其中$\eta_1>0,\eta_2>0,\eta_3>0$为可调参数.

采用如下重置算法使估计算法式(27)具有更强的对时变参数的跟踪能力:

如果$|\hat{g}_{a,ii,k}(t)|<b_2$或$|\hat{g}_{a,ii,k}(t)|>\alpha b_2$或$\mathrm{sgn}(\hat{g}_{a,ii,k}(t))\neq\mathrm{sgn}(\hat{g}_{a,ii,0}(t))$. 则

$$\hat{g}_{a,ii,k}(t)=\hat{g}_{a,ii,0}(t),\tag{28}$$

如果$|\hat{g}_{a,ij,k}(t)|>b_1$或$\mathrm{sgn}(\hat{g}_{a,ij,k}(t))\neq\mathrm{sgn}(\hat{g}_{a,ij,0}(t))$. 则

$$\hat{g}_{a,ij,k}(t)=\hat{g}_{a,ij,0}(t),\tag{29}$$

其中: $\hat{g}_{a,ii,0}(t)$, $\hat{g}_{a,ij,0}(t)$分别是$\hat{g}_{a,ii,k}(t)$, $\hat{g}_{a,ij,k}(t)$的初始次迭代t时刻的值$(a=1,2,3)$; $\alpha\geqslant1, b_1>0, b_2>0$是常数, 在假设4中有进一步的说明.

采用估计算法式(27)–(29)得PJM估计值$\hat{\boldsymbol{G}}_{a,k}(t)(a=1,2,3)$后, 通过如下预报算法获取未来$k+f$次迭代的PJM预测值$\hat{\boldsymbol{G}}_{a,k+f}(t)(f=1,2,\cdots,m)$.

$$
\begin{cases}
\hat{\boldsymbol{G}}_{1,k+f}(t) = \\
\hat{\boldsymbol{\Lambda}}_{1,k}(t)\hat{\boldsymbol{G}}_{1,k+f-1}(t) + \hat{\boldsymbol{\Lambda}}_{2,k}(t)\cdot \\
\hat{\boldsymbol{G}}_{1,k+f-2}(t) + \cdots + \hat{\boldsymbol{\Lambda}}_{n_p,k}(t)\hat{\boldsymbol{G}}_{1,k+f-n_p}(t), \\
\hat{\boldsymbol{G}}_{2,k+f}(t) = \\
\hat{\boldsymbol{M}}_{1,k}(t)\hat{\boldsymbol{G}}_{2,k+f-1}(t) + \hat{\boldsymbol{M}}_{2,k}(t)\cdot \\
\hat{\boldsymbol{G}}_{2,k+f-2}(t) + \cdots + \hat{\boldsymbol{M}}_{n_p,k}(t)\hat{\boldsymbol{G}}_{2,k+f-n_p}(t), \\
\hat{\boldsymbol{G}}_{3,k+f}(t) = \\
\hat{\boldsymbol{N}}_{1,k}(t)\hat{\boldsymbol{G}}_{3,k+f-1}(t) + \hat{\boldsymbol{N}}_{2,k}(t)\cdot \\
\hat{\boldsymbol{G}}_{3,k+f-2}(t) + \cdots + \hat{\boldsymbol{N}}_{n_p,k}(t)\hat{\boldsymbol{G}}_{3,k+f-n_p}(t),
\end{cases} \tag{30}
$$

其中: 系数矩阵 $\hat{\boldsymbol{\Lambda}}_{\varpi,k}(t), \hat{\boldsymbol{M}}_{\varpi,k}(t), \hat{\boldsymbol{N}}_{\varpi,k}(t)$ 分别是 $\boldsymbol{\Lambda}_{\varpi}(t), \boldsymbol{M}_{\varpi}(t), \boldsymbol{N}_{\varpi}(t) (\varpi = 1, 2, \cdots, n_p)$ 在第 k 次迭代的估计值. 定义

$$
\begin{cases}
\hat{\boldsymbol{\Lambda}}_k^{n_p}(t) = [\hat{\boldsymbol{\Lambda}}_{1,k}^{\mathrm{T}}(t) \ \cdots \ \hat{\boldsymbol{\Lambda}}_{n_p,k}^{\mathrm{T}}(t)]^{\mathrm{T}} \in \mathbb{R}^{nn_p \times n}, \\
\hat{\boldsymbol{M}}_k^{n_p}(t) = [\hat{\boldsymbol{M}}_{1,k}^{\mathrm{T}}(t) \ \cdots \ \hat{\boldsymbol{M}}_{n_p,k}^{\mathrm{T}}(t)]^{\mathrm{T}} \in \mathbb{R}^{nn_p \times n}, \\
\hat{\boldsymbol{N}}_k^{n_p}(t) = [\hat{\boldsymbol{N}}_{1,k}^{\mathrm{T}}(t) \ \cdots \ \hat{\boldsymbol{N}}_{n_p,k}^{\mathrm{T}}(t)]^{\mathrm{T}} \in \mathbb{R}^{nn_p \times n}, \\
\hat{\boldsymbol{\Phi}}_{a,k-1}(t) = [\hat{\boldsymbol{G}}_{a,k-1}(t) \ \cdots \ \hat{\boldsymbol{G}}_{a,k-n_p}(t)]^{\mathrm{T}} \in \\
\mathbb{R}^{nn_p \times n} (a = 1, 2, 3),
\end{cases} \tag{31}
$$

则式(30)可写为

$$
\begin{cases}
\hat{\boldsymbol{G}}_{1,k+f}(t) = \hat{\boldsymbol{\Phi}}_{1,k+f-1}^{\mathrm{T}}(t)\hat{\boldsymbol{\Lambda}}_k^{n_p}(t), \\
\hat{\boldsymbol{G}}_{2,k+f}(t) = \hat{\boldsymbol{\Phi}}_{2,k+f-1}^{\mathrm{T}}(t)\hat{\boldsymbol{M}}_k^{n_p}(t), \\
\hat{\boldsymbol{G}}_{3,k+f}(t) = \hat{\boldsymbol{\Phi}}_{3,k+f-1}^{\mathrm{T}}(t)\hat{\boldsymbol{N}}_k^{n_p}(t).
\end{cases} \tag{32}
$$

通过如下沿迭代轴的学习算法来计算$\hat{\boldsymbol{\Lambda}}_k^{n_p}(t)$, $\hat{\boldsymbol{M}}_k^{n_p}(t)$, $\hat{\boldsymbol{N}}_k^{n_p}(t)$:

$$
\begin{cases}
\hat{\boldsymbol{\Lambda}}_k^{n_p}(t) = \\
\hat{\boldsymbol{\Lambda}}_{k-1}^{n_p}(t) + \ell_1\hat{\boldsymbol{\Phi}}_{1,k-1}(t)[\sigma_1\boldsymbol{I} + \\
\hat{\boldsymbol{\Phi}}_{1,k-1}^{\mathrm{T}}(t)\hat{\boldsymbol{\Phi}}_{1,k-1}(t)]^{-1}[\hat{\boldsymbol{G}}_{1,k}(t) - \\
\hat{\boldsymbol{\Phi}}_{1,k-1}^{\mathrm{T}}(t)\hat{\boldsymbol{\Lambda}}_{k-1}^{n_p}(t)], \\
\hat{\boldsymbol{M}}_k^{n_p}(t) = \\
\hat{\boldsymbol{M}}_{k-1}^{n_p}(t) + \ell_2\hat{\boldsymbol{\Phi}}_{2,k-1}(t)[\sigma_2\boldsymbol{I} + \\
\hat{\boldsymbol{\Phi}}_{2,k-1}^{\mathrm{T}}(t)\hat{\boldsymbol{\Phi}}_{2,k-1}(t)]^{-1}[\hat{\boldsymbol{G}}_{2,k}(t) - \\
\hat{\boldsymbol{\Phi}}_{2,k-1}^{\mathrm{T}}(t)\hat{\boldsymbol{M}}_{k-1}^{n_p}(t)], \\
\hat{\boldsymbol{N}}_k^{n_p}(t) = \\
\hat{\boldsymbol{N}}_{k-1}^{n_p}(t) + \ell_3\hat{\boldsymbol{\Phi}}_{3,k-1}(t)[\sigma_3\boldsymbol{I} + \\
\hat{\boldsymbol{\Phi}}_{3,k-1}^{\mathrm{T}}(t)\hat{\boldsymbol{\Phi}}_{3,k-1}(t)]^{-1}[\hat{\boldsymbol{G}}_{3,k}(t) - \\
\hat{\boldsymbol{\Phi}}_{3,k-1}^{\mathrm{T}}(t)\hat{\boldsymbol{N}}_{k-1}^{n_p}(t)],
\end{cases} \tag{33}
$$

其中$\ell_1, \ell_2, \ell_3, \sigma_1, \sigma_2, \sigma_3$是可调的参数.

通过预报算法式(30)–(33)得到$\boldsymbol{G}_{a,k+1}^m(t)$的预报值$\hat{\boldsymbol{G}}_{a,k+1}^m(t)$后, 则式(20)可以写为

$$
\begin{aligned}
&\boldsymbol{e}_{k+m|k}^*(t+1) = \\
&\boldsymbol{e}_k^*(t+1) - \hat{\boldsymbol{G}}_{1,k+1}^m(t)\Delta\boldsymbol{u}_{k+1}^m(t) - \\
&\hat{\boldsymbol{G}}_{2,k+1}^m(t)\Delta\boldsymbol{u}_{k+1}^m(t-\tau_1(t)) - \\
&\hat{\boldsymbol{G}}_{3,k+1}^m(t)\Delta\boldsymbol{u}_{k+1}^m(t-\tau_2(t)).
\end{aligned} \tag{34}
$$

基于式(34), $\Delta\boldsymbol{u}_{k+1}^m(t)$可通过计算下面的二次成本函数获取:

$$
\begin{aligned}
&\bar{J}_{k+1}(t) = \\
&\min_{\Delta\boldsymbol{u}_{k+1}^m(t)} \{\boldsymbol{e}_{k+m|k}^{*\mathrm{T}}(t+1)\boldsymbol{Q}\boldsymbol{e}_{k+m|k}^*(t+1) + \\
&\Delta\boldsymbol{u}_{k+1}^{m\mathrm{T}}(t)\boldsymbol{R}\Delta\boldsymbol{u}_{k+1}^m(t)\},
\end{aligned} \tag{35}
$$

其中: $\boldsymbol{Q} = q\boldsymbol{I}_{n\times n}, \boldsymbol{R} = r\boldsymbol{I}_{nm\times nm}$是两个对称的正定矩阵, $q > 0, r > 0$. 根据优化条件$\dfrac{\partial \bar{J}_{k+1}(t)}{\partial \Delta\boldsymbol{u}_{k+1}^m(t)} = \boldsymbol{0}$, 可得控制输入:

$$
\begin{aligned}
&\Delta\boldsymbol{u}_{k+1}^m(t) = \\
&[\hat{\boldsymbol{G}}_{1,k+1}^{m\mathrm{T}}(t)\boldsymbol{Q}\hat{\boldsymbol{G}}_{1,k+1}^m(t) + \boldsymbol{R}]^{-1}\cdot \\
&[\hat{\boldsymbol{G}}_{1,k+1}^{m\mathrm{T}}(t)\boldsymbol{Q}\boldsymbol{e}_k^*(t+1) - \\
&\hat{\boldsymbol{G}}_{1,k+1}^{m\mathrm{T}}(t)\boldsymbol{Q}\hat{\boldsymbol{G}}_{2,k+1}^m(t)\Delta\boldsymbol{u}_{k+1}^m(t-\tau_1(t)) - \\
&\hat{\boldsymbol{G}}_{1,k+1}^{m\mathrm{T}}(t)\boldsymbol{Q}\hat{\boldsymbol{G}}_{3,k+1}^m(t)\Delta\boldsymbol{u}_{k+1}^m(t-\tau_2(t))].
\end{aligned} \tag{36}
$$

由于控制算法式(36)中含有矩阵求逆运算, 当系统输入输出维数很大时, 求逆运算非常耗时, 不利于实际应用. 为了解决这一问题, 将控制算法简化为

$$
\begin{aligned}
\Delta\boldsymbol{u}_{k+1}^m(t) = &\frac{\gamma q\hat{\boldsymbol{G}}_{1,k+1}^{m\mathrm{T}}(t)}{r + q\left\|\hat{\boldsymbol{G}}_{1,k+1}^m(t)\right\|^2}[\boldsymbol{e}_k^*(t+1) - \\
&\hat{\boldsymbol{G}}_{2,k+1}^m(t)\Delta\boldsymbol{u}_{k+1}^m(t-\tau_1(t)) - \\
&\hat{\boldsymbol{G}}_{3,k+1}^m(t)\Delta\boldsymbol{u}_{k+1}^m(t-\tau_2(t))],
\end{aligned} \tag{37}
$$

其中$0 < \gamma \leqslant 1$是步长因子, 它的引入是为了使控制算法更具一般性.

利用预测控制中的滚动优化策略, 可得

$$
\boldsymbol{u}_{k+1}(t) = \boldsymbol{u}_k(t) + \boldsymbol{U}^{\mathrm{T}}\Delta\boldsymbol{u}_{k+1}^m(t), \tag{38}
$$

其中$\boldsymbol{U} = \left[\boldsymbol{I}_{n\times n}\boldsymbol{0}_{n\times n(m-1)}\right]^{\mathrm{T}}$.

本篇论文的控制算法流程如表1所示.

表 1 控制算法流程

Table 1 Control algorithm flow

1. 对PJM $\boldsymbol{G}_{a,k}(t)$进行估计, 得到估计值$\hat{\boldsymbol{G}}_{a,k}(t) (a = 1, 2, 3)$	式(27)–(29)
2. 对PJM $\boldsymbol{G}_{a,k+f}(t)$进行预测, 得到预测值$\hat{\boldsymbol{G}}_{a,k+f}(t)$ $(a = 1, 2, 3, f = 1, \cdots, m)$	式(30–33)
3. 计算$\Delta\boldsymbol{u}_{k+1}^m(t)$以及$\boldsymbol{u}_{k+1}(t)$	式(37–38)
4. 将控制输入$\boldsymbol{u}_{k+1}(t)$应用到系统	
5. 令$k = k + 1$, 并重复以上步骤	

在给出所提控制方法的收敛性质前, 首先给出如下假设和引理.

假设 4 PJM $\boldsymbol{G}_{a,k}(t)$ $(a = 1, 2, 3)$ 是对角占优矩阵, 且满足以下条件: $|g_{a,ij,k}(t)| \leqslant b_1$, $b_2 \leqslant$

$|g_{a,ii,k}(t)| \leqslant \alpha b_2, i=1,\cdots,n, j=1,\cdots,n, i\neq j, \alpha\geqslant 1, b_2\geqslant b_1(2\alpha+1)(n-1)$且$\boldsymbol{G}_{a,k}(t)$中所有的元素符号在任意$t$时刻保持不变.

注 4 假设4是关于系统输入输出数据关系的假设, 由于所针对的系统模型未知, 仅知道系统到当前时刻为止的输入输出数据, 因此系统输入输出数据关系的对角占优条件可能是描述系统各变量之间耦合的唯一可行的选择[34–36]. 而PJM $\boldsymbol{G}_{a,k}(t)(a=1,2,3)$中元素符号的假设与很多基于模型的控制方法中的相关假设类似[37–38]. 实际上, 许多实际系统可以验证满足这一假设, 如搅拌槽系统[39]、木材/浆果蒸馏塔系统[40]、双连杆机械手系统[41]、多智能体系统[42]等.

引理 1[43] 令$\boldsymbol{A}=(x_{ij})\in\mathbb{C}^{n\times n}$, 定义Gerschgorin圆盘: $D_i=\{z||z-x_{ii}|\leqslant\sum\limits_{j=1,j\neq i}^{n}|x_{ij}|\}, z\in\mathbb{C}$, $1\leqslant i\leqslant n$. 则$\boldsymbol{A}$矩阵的所有特征根都在圆盘中, 且矩阵的所有特征根满足$z_1,z_2,\cdots,z_n\in D_A=\bigcup\limits_{i=1}^{n}D_i$.

定理 2 如果系统(1)满足假设1–4, 所提出的参数估计算法式(27)–(29), 预报算法式(30)–(33)以及控制算法式(37)–(38)满足下列条件:

$$\begin{aligned}0<\ &\eta_1\frac{\partial\tilde{e}^*_{i,k}(t+1)}{\partial\hat{\boldsymbol{G}}_{1,i,k}(t)}\Big(\frac{\partial\tilde{e}^*_{i,k}(t+1)}{\partial\hat{\boldsymbol{G}}_{1,i,k}(t)}\Big)^{\mathrm{T}}+\\&\eta_2\frac{\partial\tilde{e}^*_{i,k}(t+1)}{\partial\hat{\boldsymbol{G}}_{2,i,k}(t)}\Big(\frac{\partial\tilde{e}^*_{i,k}(t+1)}{\partial\hat{\boldsymbol{G}}_{2,i,k}(t)}\Big)^{\mathrm{T}}+\\&\eta_3\frac{\partial\tilde{e}^*_{i,k}(t+1)}{\partial\hat{\boldsymbol{G}}_{3,i,k}(t)}\Big(\frac{\partial\tilde{e}^*_{i,k}(t+1)}{\partial\hat{\boldsymbol{G}}_{3,i,k}(t)}\Big)^{\mathrm{T}}<1,\\&i=1,2,\cdots,n,\end{aligned}\tag{39}$$

其中: $\hat{\boldsymbol{G}}_{a,i,k}(a=1,2,3)$是PJM $\hat{\boldsymbol{G}}_{a,k}$的第$i$行, $\tilde{e}^*_{i,k}(t+1)(i=1,\cdots,n)$是$\tilde{\boldsymbol{e}}^*_k(t+1)$的第$i$个元素, $\hat{\boldsymbol{G}}_{a,i,k}$以及$\tilde{e}^*_{i,k}(t+1)$分别从式(8)与式(24)中获取. 则有:

1) 式(23)定义的建模误差可收敛到零. 即$\lim\limits_{k\to\infty}\tilde{\boldsymbol{e}}^*_{k+1}(t+1)=\boldsymbol{0}$.

2) 式(3)定义的跟踪控制误差可收敛到一个界内, 即$\lim\limits_{k\to\infty}\|\boldsymbol{e}^*_{k+1}(t+1)\|_v\leqslant\dfrac{c}{1-d_1}$, 其中: $0\leqslant d_1<1$从式(63)中获取, $c\geqslant 0$从式(64)中获取.

证 1) 由式(8)(23)–(25)可得

$$\begin{aligned}&\tilde{e}^*_{i,k+1}(t+1)=y^*_{i,k+1}(t+1)-\hat{y}_{i,k+1}(t+1)=\\&y^*_{i,k+1}(t+1)-y^*_{i,k}(t+1)-\hat{\boldsymbol{G}}_{1,i,k+1}(t)\Delta\boldsymbol{u}_{k+1}(t)-\\&\hat{\boldsymbol{G}}_{2,i,k+1}(t)\Delta\boldsymbol{u}_{k+1}(t-\tau_1(t))-\\&\hat{\boldsymbol{G}}_{3,i,k+1}(t)\Delta\boldsymbol{u}_{k+1}(t-\tau_2(t)).\end{aligned}\tag{40}$$

由于$y^*_{i,k+1}(t+1)$与$y^*_{i,k}(t+1)$根据补偿机制式(26)分别有4种情况的取值, 以$y^*_{i,k}(t+1)$为例, 4种情况分别是: 1) 当前第k次迭代真实的输出$y_{i,k}(t+1)$; 2) 历史$k-1$次迭代的真实的输出$y_{i,k-1}(t+1)$; 3) 历史$k-2$次迭代的真实的输出$y_{i,k-2}(t+1)$; 4) $t+1$时刻期望的输出$y_d(t+1)$.

$y^*_{i,k+1}(t+1)$与$y^*_{i,k}(t+1)$的4种情况两两结合有多种不同的补偿方式, 如$y^*_{i,k}(t+1)$取$y_{i,k}(t+1)$, $y^*_{i,k+1}(t+1)$取$y_{i,k+1}(t+1)$等, 式(41)选择其中一种来证明. 即第k次迭代$t+1$时刻没有真实的输出值但历史第$k-1$次迭代$t+1$时刻能搜到真实的输出值, 同时第$k+1$次迭代的$t+1$时刻有真实的输出值. 即$y^*_{i,k}(t+1)=y_{i,k-1}(t+1)$, $y^*_{i,k+1}(t+1)=y_{i,k+1}(t+1)$, 其他情况的选取通过类似式(41)–(51)的分析, 均能保证建模误差$\tilde{e}^*_{i,k+1}(t+1)$的收敛性, 由于篇幅限制, 这里不再详述.

基于上述分析, 式(40)可被写为

$$\begin{aligned}&\tilde{e}^*_{i,k+1}(t+1)=\\&y_{i,k+1}(t+1)-y_{i,k-1}(t+1)-\hat{\boldsymbol{G}}_{1,i,k+1}(t)\cdot\\&\Delta\boldsymbol{u}_{k+1}(t)-\hat{\boldsymbol{G}}_{2,i,k+1}(t)\Delta\boldsymbol{u}_{k+1}(t-\tau_1(t))-\\&\hat{\boldsymbol{G}}_{3,i,k+1}(t)\Delta\boldsymbol{u}_{k+1}(t-\tau_2(t)).\end{aligned}\tag{41}$$

定义如下复合能量函数:

$$E^*_{i,k+1}(t+1)=\tilde{e}^*_{i,k+1}(t+1)^2,\ i=1,2,\cdots,n,\tag{42}$$

则其在迭代轴上的差分可表示为

$$\begin{aligned}&\Delta E^*_{i,k+1}(t+1)=\\&E^*_{i,k+1}(t+1)-E^*_{i,k}(t+1)=\\&\tilde{e}^*_{i,k+1}(t+1)^2-\tilde{e}^*_{i,k}(t+1)^2=\\&\Delta\tilde{e}^*_{i,k+1}(t+1)^2+2\tilde{e}^*_{i,k}(t+1)\Delta\tilde{e}^*_{i,k+1}(t+1),\end{aligned}\tag{43}$$

其中$\Delta\tilde{e}^*_{i,k+1}(t+1)=\tilde{e}^*_{i,k+1}(t+1)-\tilde{e}^*_{i,k}(t+1)$.

对$\Delta\tilde{e}^*_{i,k+1}(t+1)$应用泰勒展开可得

$$\begin{aligned}&\Delta\tilde{e}^*_{i,k+1}(t+1)=\\&\frac{\partial\tilde{e}^*_{i,k}(t+1)}{\partial\hat{\boldsymbol{G}}_{1,i,k}(t)}\Delta\hat{\boldsymbol{G}}^{\mathrm{T}}_{1,i,k+1}(t)+\\&\frac{\partial\tilde{e}^*_{i,k}(t+1)}{\partial\hat{\boldsymbol{G}}_{2,i,k}(t)}\Delta\hat{\boldsymbol{G}}^{\mathrm{T}}_{2,i,k+1}(t)+\\&\frac{\partial\tilde{e}^*_{i,k}(t+1)}{\partial\hat{\boldsymbol{G}}_{3,i,k}(t)}\Delta\hat{\boldsymbol{G}}^{\mathrm{T}}_{3,i,k+1}(t),\end{aligned}\tag{44}$$

其中$\Delta\hat{\boldsymbol{G}}^{\mathrm{T}}_{a,i,k+1}(t)=\hat{\boldsymbol{G}}^{\mathrm{T}}_{a,i,k+1}(t)-\hat{\boldsymbol{G}}^{\mathrm{T}}_{a,i,k}(t)(a=1,2,3)$.

把式(27)带入式(44)可得

$$\begin{aligned}&\Delta\tilde{e}^*_{i,k+1}(t+1)=\\&\eta_1\frac{\partial\tilde{e}^*_{i,k}(t+1)}{\partial\hat{\boldsymbol{G}}_{1,i,k}(t)}\tilde{e}^*_{i,k}(t+1)\Delta\boldsymbol{u}_k(t)+\\&\eta_2\frac{\partial\tilde{e}^*_{i,k}(t+1)}{\partial\hat{\boldsymbol{G}}_{2,i,k}(t)}\tilde{e}^*_{i,k}(t+1)\Delta\boldsymbol{u}_k(t-\tau_1(t))+\end{aligned}$$

$$\eta_3\frac{\partial\tilde{e}^*_{i,k}(t+1)}{\partial\hat{\boldsymbol{G}}_{3,i,k}(t)}\tilde{e}^*_{i,k}(t+1)\Delta\boldsymbol{u}_k(t-\tau_2(t)). \quad (45)$$

由式(41)和式(45)可得

$$\Delta\tilde{e}^*_{i,k+1}(t+1)=-\tilde{e}^*_{i,k}(t+1)l_{i,k}(t+1), \quad (46)$$

其中

$$\begin{aligned}l_{i,k}(t+1)=&\eta_1\frac{\partial\tilde{e}^*_{i,k}(t+1)}{\partial\hat{\boldsymbol{G}}_{1,i,k}(t)}(\frac{\partial\tilde{e}^*_{i,k}(t+1)}{\partial\hat{\boldsymbol{G}}_{1,i,k}(t)})^{\mathrm{T}}+\\&\eta_2\frac{\partial\tilde{e}^*_{i,k}(t+1)}{\partial\hat{\boldsymbol{G}}_{2,i,k}(t)}(\frac{\partial\tilde{e}^*_{i,k}(t+1)}{\partial\hat{\boldsymbol{G}}_{2,i,k}(t)})^{\mathrm{T}}+\\&\eta_3\frac{\partial\tilde{e}^*_{i,k}(t+1)}{\partial\hat{\boldsymbol{G}}_{3,i,k}(t)}(\frac{\partial\tilde{e}^*_{i,k}(t+1)}{\partial\hat{\boldsymbol{G}}_{3,i,k}(t)})^{\mathrm{T}}.\end{aligned} \quad (47)$$

将式(46)代入式(43)可得

$$\begin{aligned}&\Delta E^*_{i,k+1}(t+1)=\\&\Delta\tilde{e}^*_{i,k+1}(t+1)^2+2\tilde{e}^*_{i,k}(t+1)\Delta\tilde{e}^*_{i,k+1}(t+1)=\\&\tilde{e}^*_{i,k}(t+1)^2[l_{i,k}(t+1)^2-2l_{i,k}(t+1)],\end{aligned} \quad (48)$$

根据条件(39)可知$0<l_{i,k}(t+1)<1$, 则由式(43)和式(48)可得

$$\Delta E^*_{i,k+1}(t+1)\leqslant-l_{i,k}(t+1)\tilde{e}^*_{i,k}(t+1)^2, \quad (49)$$

根据式(43)进一步有

$$\tilde{e}^*_{i,k+1}(t+1)^2\leqslant[1-l_{i,k}(t+1)]\,\tilde{e}^*_{i,k}(t+1)^2, \quad (50)$$

根据条件(39), 存在正常数ρ满足$0<1-l_{i,k}(t+1)\leqslant\rho<1$, 式(50)可被简化为

$$\tilde{e}^*_{i,k+1}(t+1)^2\leqslant\rho\tilde{e}^*_{i,k}(t+1)^2, \quad (51)$$

于是有$\lim\limits_{k\to\infty}\tilde{\boldsymbol{e}}^*_{k+1}(t+1)=\boldsymbol{0}$.

2) 根据控制律式(37)–(38)与式(14)可得

$$\begin{aligned}&\boldsymbol{e}^*_{k+1}(t+1)=\\&\boldsymbol{e}^*_k(t+1)-\frac{\gamma q\boldsymbol{G}_{1,k+1}(t)\boldsymbol{U}^{\mathrm{T}}\hat{\boldsymbol{G}}^{m\mathrm{T}}_{1,k+1}(t)}{r+q\|\hat{\boldsymbol{G}}^m_{1,k+1}(t)\|^2}\boldsymbol{e}^*_k(t+1)+\\&\frac{\gamma q\boldsymbol{G}_{1,k+1}(t)\boldsymbol{U}^{\mathrm{T}}\hat{\boldsymbol{G}}^{m\mathrm{T}}_{1,k+1}(t)}{r+q\|\hat{\boldsymbol{G}}^m_{1,k+1}(t)\|^2}\cdot\\&[\hat{\boldsymbol{G}}^m_{2,k+1}(t)\Delta\boldsymbol{u}^m_{k+1}(t-\tau_1(t))+\\&\hat{\boldsymbol{G}}^m_{3,k+1}(t)\Delta\boldsymbol{u}^m_{k+1}(t-\tau_2(t))]-\\&\boldsymbol{G}_{2,k+1}(t)\Delta\boldsymbol{u}_{k+1}(t-\tau_1(t))-\\&\boldsymbol{G}_{3,k+1}(t)\Delta\boldsymbol{u}_{k+1}(t-\tau_2(t))=\\&\boldsymbol{C}+\{\boldsymbol{I}-\frac{\gamma q\boldsymbol{G}_{1,k+1}(t)\hat{\boldsymbol{G}}^{\mathrm{T}}_{1,k+1}(t)}{r+q\|\hat{\boldsymbol{G}}^m_{1,k+1}(t)\|^2}\}\boldsymbol{e}^*_k(t+1),\end{aligned} \quad (52)$$

其中

$$\begin{aligned}&\boldsymbol{C}=\\&\frac{\gamma q\boldsymbol{G}_{1,k+1}(t)\hat{\boldsymbol{G}}^{\mathrm{T}}_{1,k+1}(t)}{r+q\|\hat{\boldsymbol{G}}^m_{1,k+1}(t)\|^2}[\hat{\boldsymbol{G}}^m_{2,k+1}(t)\cdot\\&\Delta\boldsymbol{u}^m_{k+1}(t-\tau_1(t))+\hat{\boldsymbol{G}}^m_{3,k+1}(t)\Delta\boldsymbol{u}^m_{k+1}(t-\tau_2(t))]-\\&\boldsymbol{G}_{2,k+1}(t)\Delta\boldsymbol{u}_{k+1}(t-\tau_1(t))-\\&\boldsymbol{G}_{3,k+1}(t)\Delta\boldsymbol{u}_{k+1}(t-\tau_2(t)).\end{aligned} \quad (53)$$

由引理1可得

$$\begin{aligned}&D_j=\\&\{z\|z-1+\frac{\gamma q\sum\limits_{i=1}^{n}g_{1,ji,k+1}(t)\hat{g}_{1,ji,k+1}(t)}{r+q\|\hat{\boldsymbol{G}}^m_{1,k+1}(t)\|^2}|\leqslant\\&\sum_{l=1,l\neq j}^{n}|\frac{\gamma q\sum\limits_{i=1}^{n}g_{1,ji,k+1}(t)\hat{g}_{1,li,k+1}(t)}{r+q\|\hat{\boldsymbol{G}}^m_{1,k+1}(t)\|^2}|\},\end{aligned} \quad (54)$$

其中: z是矩阵$\boldsymbol{I}-\dfrac{\gamma q\boldsymbol{G}_{1,k+1}(t)\hat{\boldsymbol{G}}^{\mathrm{T}}_{1,k+1}(t)}{r+q\|\hat{\boldsymbol{G}}^m_{1,k+1}(t)\|^2}$的特征根; $D_j, j=1,\cdots,m$, 是Gerschgorin圆盘.

利用三角不等式, 式(54)可写为

$$\begin{aligned}&D_j=\\&\{z\|z|\leqslant|1-\frac{\gamma q\sum\limits_{i=1}^{n}g_{1,ji,k+1}(t)\hat{g}_{1,ji,k+1}(t)}{r+q\|\hat{\boldsymbol{G}}^m_{1,k+1}(t)\|^2}|+\\&\sum_{l=1,l\neq j}^{n}|\frac{\gamma q\sum\limits_{i=1}^{n}g_{1,ji,k+1}(t)\hat{g}_{1,li,k+1}(t)}{r+q\|\hat{\boldsymbol{G}}^m_{1,k+1}(t)\|^2}|\}.\end{aligned} \quad (55)$$

由重置算法式(28)–(29)和假设4可以得到以下两个不等式:

$$\begin{aligned}&1-\frac{\gamma q\sum\limits_{i=1}^{n}\|g_{1,ji,k+1}(t)\|\hat{g}_{1,ji,k+1}(t)|}{r+q\|\hat{\boldsymbol{G}}^m_{1,k+1}(t)\|^2}\leqslant\\&1-\frac{\gamma q|g_{1,jj,k+1}(t)\|\hat{g}_{1,jj,k+1}(t)|}{r+q\|\hat{\boldsymbol{G}}^m_{1,k+1}(t)\|^2}\leqslant\\&1-\frac{\gamma qb_2^2}{r+q\|\hat{\boldsymbol{G}}^m_{1,k+1}(t)\|^2}\end{aligned} \quad (56)$$

和

$$\begin{aligned}&\sum_{l=1,l\neq j}^{n}\frac{\gamma q\sum\limits_{i=1}^{n}g_{1,ji,k+1}(t)\hat{g}_{1,li,k+1}(t)}{r+q\|\hat{\boldsymbol{G}}^m_{1,k+1}(t)\|^2}\leqslant\\&\gamma q\sum_{l=1,l\neq j}^{n}\frac{\sum\limits_{i=1}^{n}|g_{1,ji,k+1}(t)|\,|\hat{g}_{1,li,k+1}(t)|}{r+q\|\hat{\boldsymbol{G}}^m_{1,k+1}(t)\|^2}\leqslant\\&\gamma q\frac{\sum\limits_{l=1,l\neq j}^{n}|g_{1,jj,k+1}(t)|\,|\hat{g}_{1,lj,k+1}(t)|}{r+q\|\hat{\boldsymbol{G}}^m_{1,k+1}(t)\|^2}+\\&\gamma q\sum_{l=1,l\neq j}^{n}\frac{\sum\limits_{i=1,i\neq j}^{n}|g_{1,ji,k+1}(t)|\,|\hat{g}_{1,li,k+1}(t)|}{r+q\|\hat{\boldsymbol{G}}^m_{1,k+1}(t)\|^2}\leqslant\end{aligned}$$

$$\gamma q\frac{\sum\limits_{l=1,l\neq j}^{n}|g_{1,jj,k+1}(t)|\,|\hat{g}_{1,lj,k+1}(t)|}{r+q\|\hat{\boldsymbol{G}}_{1,k+1}^{m}(t)\|^2}+$$
$$\gamma q\frac{\sum\limits_{l=1,l\neq j}^{n}|g_{1,jl,k+1}(t)|\,|\hat{g}_{1,ll,k+1}(t)|}{r+q\|\hat{\boldsymbol{G}}_{1,k+1}^{m}(t)\|^2}+$$
$$\gamma q\sum_{l=1,l\neq j}^{n}\frac{\sum\limits_{i=1,i\neq j,l}^{n}|g_{1,ji,k+1}(t)|\,|\hat{g}_{1,li,k+1}(t)|}{r+q\|\hat{\boldsymbol{G}}_{1,k+1}^{m}(t)\|^2}\leqslant$$
$$\gamma q\frac{2\alpha b_1b_2(n-1)+b_1^2(n-1)(n-2)}{r+q\|\hat{\boldsymbol{G}}_{1,k+1}^{m}(t)\|^2}. \tag{57}$$

将式(56)和式(57)相加可得

$$1-\frac{\gamma q\sum\limits_{i=1}^{n}|g_{1,ji,k+1}(t)|\,|\hat{g}_{1,ji,k+1}(t)|}{r+q\big\|\hat{\boldsymbol{G}}_{1,k+1}^{m}(t)\big\|^2}+$$
$$\sum_{l=1,l\neq j}^{n}\frac{\gamma q\sum\limits_{i=1}^{n}g_{1,ji,k+1}(t)\hat{g}_{1,li,k+1}(t)}{r+q\big\|\hat{\boldsymbol{G}}_{1,k+1}^{m}(t)\big\|^2}\leqslant$$
$$1-\frac{\gamma qb_2^2}{r+q\big\|\hat{\boldsymbol{G}}_{1,k+1}^{m}(t)\big\|^2}+$$
$$\gamma q\frac{2\alpha b_1b_2(n-1)+b_1^2(n-1)(n-2)}{r+q\big\|\hat{\boldsymbol{G}}_{1,k+1}^{m}(t)\big\|^2}\leqslant$$
$$1-\gamma q\frac{b_2^2-2\alpha b_1b_2(n-1)-b_1^2(n-1)(n-2)}{r+q\big\|\hat{\boldsymbol{G}}_{1,k+1}^{m}(t)\big\|^2}\leqslant$$
$$1-\gamma q\frac{2\alpha b_1^2(n-1)^2}{r+q\big\|\hat{\boldsymbol{G}}_{1,k+1}^{m}(t)\big\|^2}. \tag{58}$$

由重置算法式(28)–(29)和假设4有: $g_{1,ji,k+1}(t)\cdot\hat{g}_{1,ji,k+1}(t)>0$. 因此, 存在一个$r_{\min}>0$, 当$r>r_{\min}$时, 下式成立:

$$\frac{\sum\limits_{i=1}^{n}g_{1,ji,k+1}(t)\hat{g}_{1,ji,k+1}(t)}{r+q\big\|\hat{\boldsymbol{G}}_{1,k+1}^{m}(t)\big\|^2}\leqslant\frac{\alpha^2b_2^2+b_1^2(n-1)}{r+q\big\|\hat{\boldsymbol{G}}_{1,k+1}^{m}(t)\big\|^2}\leqslant$$
$$\frac{\alpha^2b_2^2+b_1^2(n-1)}{r_{\min}+q\big\|\hat{\boldsymbol{G}}_{1,k+1}^{m}(t)\big\|^2}<1. \tag{59}$$

当$r>r_{\min}>0$和$0<\gamma q\leqslant 1$时, 下式成立:

$$0<M\leqslant\frac{2\alpha b_1^2(n-1)^2}{r+q\big\|\hat{\boldsymbol{G}}_{1,k+1}^{m}(t)\big\|^2}<$$
$$\frac{b_2^2}{r+q\big\|\hat{\boldsymbol{G}}_{1,k+1}^{m}(t)\big\|^2}\leqslant\frac{\alpha^2b_2^2+b_1^2(n-1)}{r+q\big\|\hat{\boldsymbol{G}}_{1,k+1}^{m}(t)\big\|^2}<$$
$$\frac{\alpha^2b_2^2+b_1^2(n-1)}{r_{\min}+q\big\|\hat{\boldsymbol{G}}_{1,k+1}^{m}(t)\big\|^2}<1, \tag{60}$$

其中$M>0$是一个正常数.

由式(58)和式(60)可得

$$\Big|1-\frac{\gamma q\sum\limits_{i=1}^{n}g_{1,ji,k+1}(t)\hat{g}_{1,ji,k+1}(t)}{r+q\big\|\hat{\boldsymbol{G}}_{1,k+1}^{m}(t)\big\|^2}\Big|+$$
$$\sum_{l=1,l\neq j}^{n}\frac{\gamma q\sum\limits_{i=1}^{n}g_{1,ji,k+1}(t)\hat{g}_{1,li,k+1}(t)}{r+q\big\|\hat{\boldsymbol{G}}_{1,k+1}^{m}(t)\big\|^2}=$$
$$1-\frac{\gamma q\sum\limits_{i=1}^{n}\big|g_{1,ji,k+1}(t)\big|\big|\hat{g}_{1,ji,k+1}(t)\big|}{r+q\big\|\hat{\boldsymbol{G}}_{1,k+1}^{m}(t)\big\|^2}+$$
$$\sum_{l=1,l\neq j}^{n}\frac{\gamma q\sum\limits_{i=1}^{n}g_{1,ji,k+1}(t)\hat{g}_{1,li,k+1}(t)}{r+q\big\|\hat{\boldsymbol{G}}_{1,k+1}^{m}(t)\big\|^2}<$$
$$1-\frac{\gamma q2\alpha b_1^2(n-1)^2}{r+q\big\|\hat{\boldsymbol{G}}_{1,k+1}^{m}(t)\big\|^2}<1-\gamma qM<1. \tag{61}$$

由式(55)和式(61)可得

$$s(\boldsymbol{I}-\frac{\gamma q\boldsymbol{G}_{1,k+1}(t)\hat{\boldsymbol{G}}_{1,k+1}^{\mathrm{T}}(t)}{r+q\big\|\hat{\boldsymbol{G}}_{1,k+1}^{m}(t)\big\|^2})<$$
$$1-\gamma qM<1, \tag{62}$$

其中: $s(\boldsymbol{A})$是矩阵$\boldsymbol{A}$的谱半径, 即: $s(\boldsymbol{A})=\max\limits_{s\in\{1,2,\cdots,m\}}|z_s|$, $z_s(s=1,2,\cdots,m)$是矩阵$\boldsymbol{A}$的特征值.

由矩阵的谱半径的知识可得, 存在任意小的$\varepsilon>0$, 使得下式成立:

$$0\leqslant\big\|\boldsymbol{I}-\frac{\gamma q\boldsymbol{G}_{1,k+1}(t)\hat{\boldsymbol{G}}_{1,k+1}^{\mathrm{T}}(t)}{r+q\big\|\hat{\boldsymbol{G}}_{1,k+1}^{m}(t)\big\|^2}\big\|_v\leqslant$$
$$s(\boldsymbol{I}-\frac{\gamma q\boldsymbol{G}_{1,k+1}(t)\hat{\boldsymbol{G}}_{1,k+1}^{T}(t)}{r+q\big\|\hat{\boldsymbol{G}}_{1,k+1}^{m}(t)\big\|^2})+\varepsilon\leqslant$$
$$1-\gamma qM+\varepsilon\leqslant d_1<1, \tag{63}$$

其中$\big\|\boldsymbol{A}\big\|_v$是矩阵$\boldsymbol{A}$的相容范数.

对式(52)两端取相容范数可得

$$\|\boldsymbol{e}_{k+1}^{*}(t+1)\|_v\leqslant$$
$$\|\boldsymbol{I}-\frac{\gamma q\boldsymbol{G}_{1,k+1}(t)\hat{\boldsymbol{G}}_{1,k+1}^{\mathrm{T}}(t)}{r+q\|\hat{\boldsymbol{G}}_{1,k+1}^{m}(t)\|^2}\|_v\|\boldsymbol{e}_{k}^{*}(t+1)\|_v+c\leqslant$$
$$d_1\|\boldsymbol{e}_{k}^{*}(t+1)\|_v+c\leqslant\cdots\leqslant$$
$$d_1^{k+1}\big\|\boldsymbol{e}_{0}^{*}(t+1)\big\|_v+\frac{c(1-d_1^k)}{1-d_1}, \tag{64}$$

其中c为式(53)取相容范数后的结果.

由$0\leqslant d_1<1$, 式(64)可写为

$$\lim_{k\to\infty}\big\|\boldsymbol{e}_{k+1}^{*}(t+1)\big\|_v\leqslant$$
$$\lim_{k\to\infty}d_1^{k+1}\big\|\boldsymbol{e}_{0}^{*}(t+1)\big\|_v+\frac{c(1-d_1^k)}{1-d_1}, \tag{65}$$

将式(65)简化为

$$\lim_{k\to\infty}\big\|\boldsymbol{e}_{k+1}^{*}(t+1)\big\|_v\leqslant\frac{c}{1-d_1}. \tag{66}$$

从不等式(66)可得当$k\to\infty$时跟踪误差$\boldsymbol{e}_{k+1}^*(t+1)$可收敛到界$\dfrac{c}{1-d_1}$内.　　证毕.

4 仿真

为了验证所提算法的有效性, 考虑如下含未知时滞的电机模型[44]:

$$\begin{cases}\dot{x}(t)=v(t),\\ \dot{v}(t)=\dfrac{u(t-h(t))-f_{\rm fric}(t)-f_{\rm rip}(t)}{m},\\ f_{\rm fric}(t)=\\ [f_c+(f_s-f_c){\rm e}^{-(v/v_s)^2}+f_v v]{\rm sgn}(v),\\ f_{\rm rip}(t)=A_r{\rm sin}(\omega_0\displaystyle\int_0^t v(\tau){\rm d}\tau),\end{cases} \tag{67}$$

其中: $x(t)$为位置, $v(t)$为速度, $u(t)$为推力, $f_{\rm fric}$为摩擦力, $f_{\rm rip}$为推力脉冲, m为质量, f_s为静态摩擦力, f_c为库仑摩擦力的最小值, v_s为润滑参数, f_v为粘滞摩擦系数, A_r和ω_0是推力脉冲中的两个参数. 电机模型的仿真参数设置为: $m=0.59$ kg, $f_c=10$ N, $f_s=20$ N, $v_s=0.01$ m/s, $f_v=10$ N·s·m^{-1}, $A_r=8.5$ N, $\omega_0=314$ rad/s, 采样周期为1 s. 时滞设置为: $h(t)=4, t\in[600,1200)$; $h(t)=2, t\in[200,400)\cup[2000,3000]$; $h(t)=1, t\in[400,800)$; $h(t)=3, t\in[800,1200)\cup[1600,2000)$; $h(t)=5, t\in[1200,1600)$, 上述时滞不参与控制器的设计.

注 5　电机模型(67)仅是为了产生系统的输入输出数据, 且控制器的设计不使用电机模型的任何结构与参数信息.

在仿真中, 将电机的速度$v(t)$作为系统的输出, 电机所跟踪的的期望轨迹为

$$y_d(t)=2{\rm sin}^2(\pi t/600),\ 0\leqslant t\leqslant 3000, \tag{68}$$

仿真中系统实际的运行时间长度在区间[2500, 3200]范围内随机变化, 如图2所示. 本文所提控制算法式(37)–(38), 参数估计算法式(27)–(29), 以及预报算法式(30)–(33)的参数设置为: $r=0.15$, $q=0.95$, $\alpha=10^3$, $b_1=10^{-7}$, $b_2=0.9\times10^{-3}$, $\eta_1=0.1$, $\eta_2=0.1$, $\eta_3=0.1$, $\gamma=0.5$, $\ell_1=1$, $\ell_2=1$, $\ell_3=1$, $\sigma_1=0.5$, $\sigma_2=0.5$, $\sigma_3=0.5$, $n_p=2$, $\hat{G}_{1,0}=0.5$, $\hat{G}_{1,1}=0.5$, $\hat{G}_{2,0}=0.5$, $\hat{G}_{2,1}=0.5$, $\hat{G}_{3,0}=0.5$, $\hat{G}_{3,1}=0.5$, $\Lambda_{1,0}=0.2$, $\Lambda_{1,1}=0.2$, $\Lambda_{2,0}=0.2$, $\Lambda_{2,1}=0.2$, $N_{1,0}=0.2$, $N_{1,1}=0.2$, $N_{2,0}=0.2$, $N_{2,1}=0.2$, $M_{1,0}=0.2$, $M_{1,1}=0.2$, $M_{2,0}=0.2$, $M_{2,1}=0.2$.

上述参数是保证系统在迭代轴上不发散且使控制性能最优的参数. 为了展示本文所提算法处理时滞的能力, 将时滞上下界设置为: $\tau_1(t)=1, t\in[0,3000]$, $\tau_2(t)=5, t\in[0,1200)$, $\tau_2(t)=6, t\in[1200,3000]$.

此外, 将本文所提算法分别与文献[27]中的高阶ILC算法、时间域上经典的PD控制算法、经典PD型ILC算法, 以及文献[20]中基于模型的多点预测ILC算法进行比较.

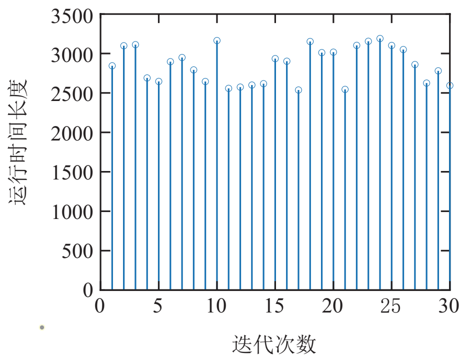

图 2　30次迭代的运行时间长度

Fig. 2　Varying trial lengths of 30 iterations

文献[27]中的高阶ILC控制器为

$$u_{k+1}(t)=\sum_{i=1}^N W_i u_{k-i+1}(t)+\sum_{i=1}^N L_i e_{k-i+1}(t+1),$$

参数设置为: $N=2$, $W_1=0.5$, $W_2=0.5$, $L_1=-0.15$, $L_2=0.3$.

PD控制器为

$$u_{k+1}(t)=D_1[e_{k+1}(t)-e_{k+1}(t-1)]+L_1e_{k+1}(t),$$

参数设置为$D_1=10$, $L_1=-1$.

PD型ILC控制器为

$$u_{k+1}(t)=u_k(t)+D_2[e_k(t+1)-e_k(t)]+L_2e_k(t+1),$$

参数设置为$D_2=0.04$, $L_2=0.12$.

上述3种算法若系统实际运行的时刻$T_k<T_d$时, 则将区间$(T_k,T_d]$缺失的数据进行补零.

文献[20]中的多点模型预测ILC控制器为

$$u_{k+1}(t)=\frac{G_u\left[y_d(t+1)-G_xy_{k+1}(t)-e_{p_k}(t)\right]}{L+G_u^2}+\frac{L\sum\limits_{i=1}^{t_e-t_s+1}w_i(u_k(t_s+i-1))}{L+G_u^2},$$

其中: L是可调的控制参数; $G_u=B, G_x=A$是线性化后系统模型参数; 根据电机模型式(67)可得$A=1, B=0.0119$. $e_{p_k}(t)$是线性化后的建模误差且$e_{p_k}(t)=y_k(t+1)-G_xy_k(t)-G_uu_k(t)$, $t_s=\max\{t-l_w,1\}$, $t_e=\min\{t-l_w,T_d\}$, l_w是预测窗口的大小, w_i是权重系数且$\sum_{i=1}^{t_e-t_s+1}w_i=1$. 仿真中参数的选取为: $L=0.0004$, $l_w=20$, $w_i(i=1,2,\cdots,t_e-t_s+1)$的取值均为$\dfrac{1}{t_e-t_s+1}$.

上述4种所比较的算法所设置的参数同样也是保证系统在迭代轴上不发散且使控制性能最优的参数.

图3为本文所提算法和文献[27]中的高阶ILC算法、PD控制算法、PD型ILC算法以及文献[20]中的多

点模型预测ILC算法的跟踪误差曲线图. 从图中可以看出, 由于时域的PD控制算法没有学习机制, 因此无论系统重复运行多少次, 误差均得不到改善. PD型ILC算法和文献[27]中高阶ILC算法中没有对未知的时滞和缺失的数据进行有效的补偿. 因此, 相较于本文所提算法, 收敛速度较慢. 而文献[20]中的多点模型预测ILC算法, 由于其控制器中利用了较多的历史运行时刻的输入数据信息, 且在仿真时使用了本文所提出的丢失数据补偿方法, 因此, 在初始的几次迭代中控制效果较优, 但其控制方法需要利用已知且时不变的系统模型参数. 而本文所提方法中系统模型参数是未知且可不断自适应更新与学习的, 因此随着迭代次数的增加, 能够获得相对更优的控制效果.

此外, 将本文对时滞的处理方法与文献[29]进行对比, 利用文献[29]对时滞的处理方法设计跟踪控制器如下:

$$u_k(t+1) = \\ k_z(\mathrm{e}^{Ah(t)}e_k(t+1)+\sum_{s=t-h(t)}^{t}\mathrm{e}^{A(t-s)}Bu_k(s)). \quad (69)$$

根据电机模型式(67)可得$A=1$, $B=0.0119$, 其中k_z为可调控制增益.

图4为本文所提算法以及文献[29]在不同时滞下的跟踪误差曲线图, 图4(a)为时滞$h(t)=2$下本文所提算法以及文献[29]在增益k_z为0.38, 0.40, 0.42情况下的跟踪误差曲线图. 从图中可以看出当$k_z=0.40$时跟踪效果最好, 当增益k_z增加或减少都会使跟踪误差变大, 因此增益$k_z=0.40$为时滞$h(t)=2$下的最优参数. 图4(b)以及图4(c)选取最优增益k_z的方法与图4(a) 的方法相同. 图 4(b) 为时滞 $h(t)=4$, $t\in[600, 1200)\cup[1800,2400)$; $h(t)=5$, $t\in$其他时刻下本文所提算法以及文献[29]在增益k_z为0.019, 0.021, 0.023情况下的跟踪误差曲线图. 图4(c)为采用本文所提时滞下本文所提算法以及文献[29]在增益k_z为0.015, 0.020, 0.025情况下的跟踪误差曲线图. 与文献[29]方法不同, 本文所提方法充分利用时滞的上下界信息对未知的时滞进行补偿, 且控制器的增益可看做是迭代可调整的. 因此, 在保持仿真参数不变的情况下, 不管未知的时滞如何变化, 所提方法均能够实现比文献[29]更小的跟踪误差.

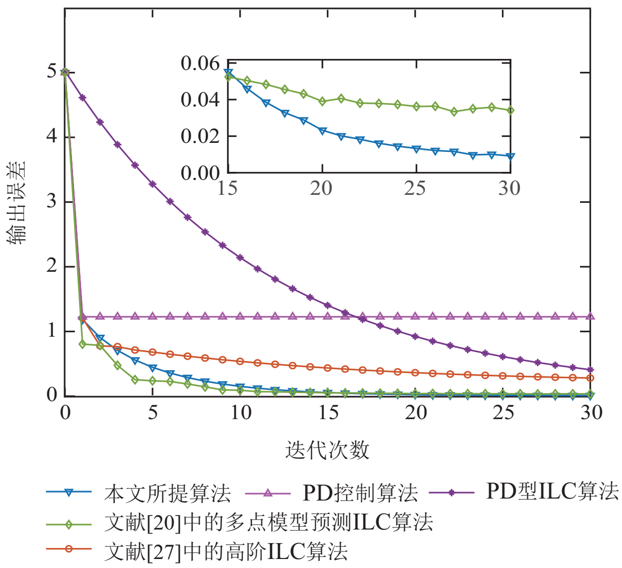

图 3 本文所提算法、文献[27]中的高阶ILC算法、PD控制算法、PD型ILC算法, 以及文献[20]中的多点模型预测ILC算法的跟踪误差曲线

Fig. 3 Tracking error curves of proposed algorithm in this paper, higher-order ILC algorithm in [27], PD control algorithm, PD-type ILC algorithm, and multi-point iterative learning model predictive control algorithm in [20]

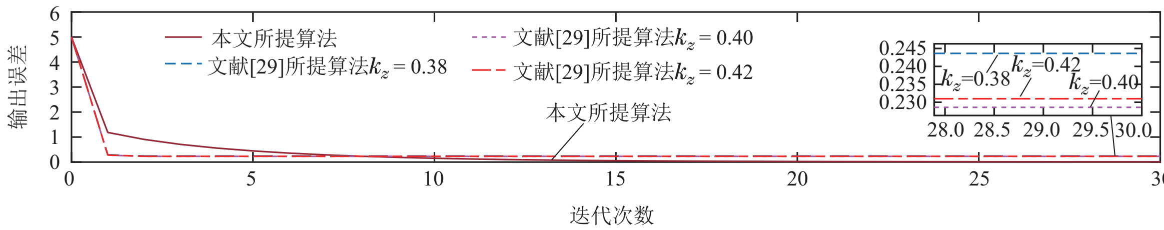

(a) 时滞$h(t)=2$, $t\in[0,3000]$

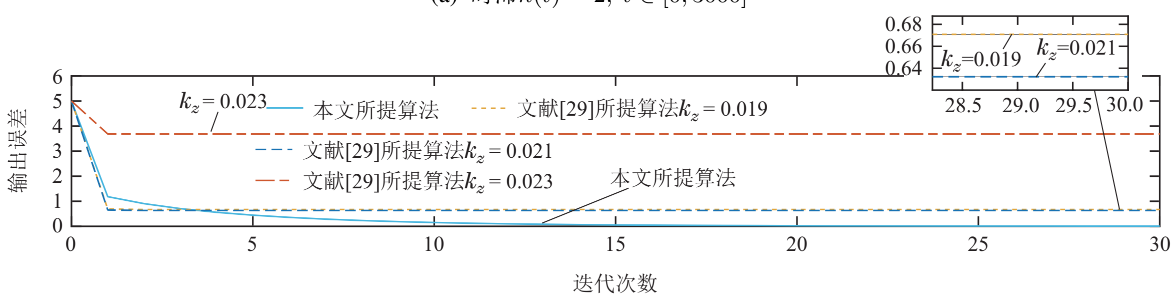

(b) 时滞$h(t)=4$, $t\in(600,1200)\cup[1800,2400]$; $h(t)=5\in$其他时刻

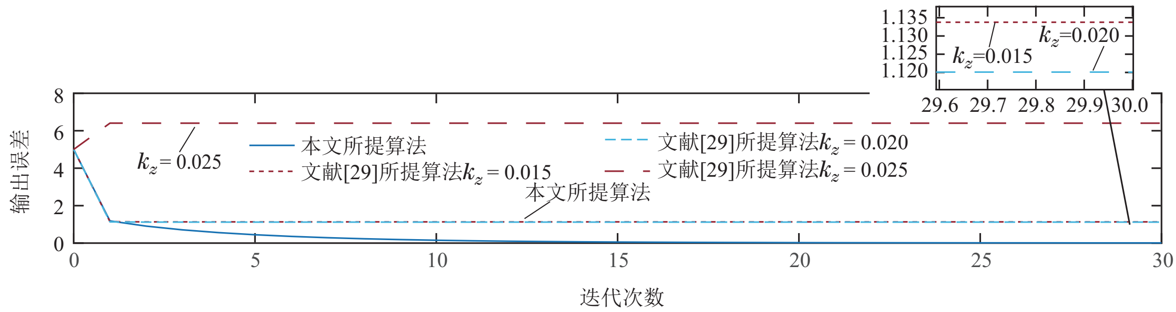

(c) $h(t)=4$采用本文所提时滞

图 4 本文所提算法以及文献[29]在不同时滞下的跟踪误差曲线

Fig. 4 Tracking error curves under different delays in [29] and proposed algorithm in this paper

图5是本文所提算法在运行时间区间变化的情况下的实际输出与期望输出的曲线图, 其中图5(a)是第15次迭代的实际输出与期望输出的曲线图, 图5(b)是第30次迭代的实际输出与期望输出的曲线图.

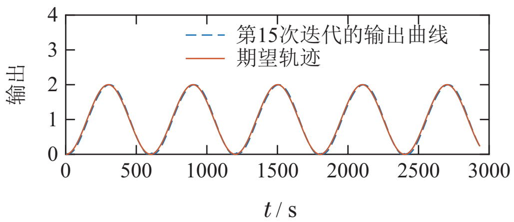

(a) 第15次迭代的输出曲线和期望输出曲线

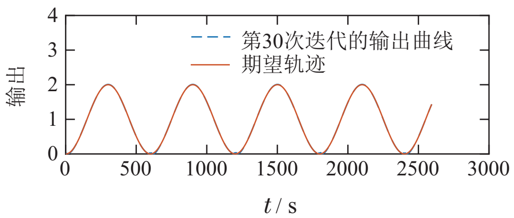

(b) 第30次迭代的输出曲线和期望输出曲线

图 5 本文所提算法第15次与第30次迭代时的实际输出曲线与期望曲线

Fig. 5 Actual and desired output curves of the proposed algorithm at the 15th and 30th iterations

图6是在本文所提算法下系统在第15次迭代和第30次迭代的控制输入, 其中图6(a)是第15次迭代的控制输入, 图6(b)是第30次迭代的控制输入. 从图5可以看出随着迭代次数的增加, 跟踪性能越好. 图3–6较好地展示了本文所提算法的跟踪控制性能, 图7将进一步展示所提算法的建模性能.

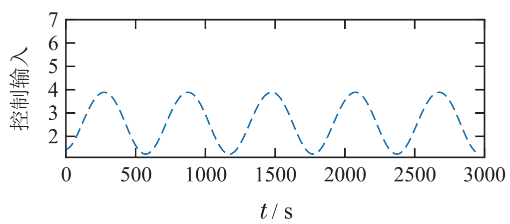

(a) 第15次迭代的控制输入

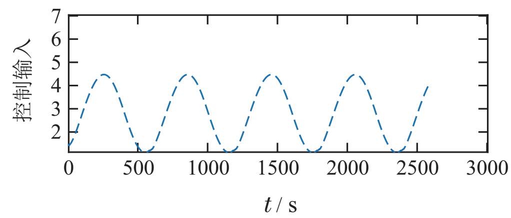

(b) 第30次迭代的控制输入

图 6 本文所提算法第15次与第30次迭代时的控制输入

Fig. 6 Control inputs of the proposed algorithm at the 15th and 30th iterations

图7是第30次迭代运行的建模误差图, 建模误差由文中式(23)定义. 从图7可以看出建模误差随着迭代次数的增加逐渐减小, 建模精度随着迭代次数的增加逐渐提高.

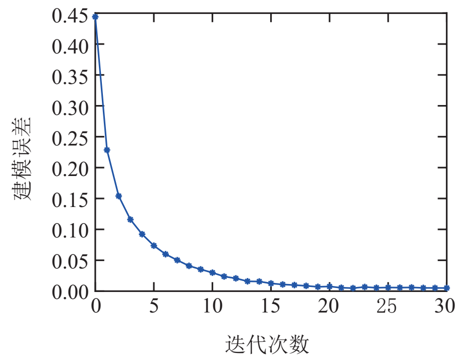

图 7 本文所提算法在迭代域上的建模误差

Fig. 7 Modeling errors of the proposed algorithm on the iterative domain

5 结论

本文针对系统模型未知的非线性非仿射离散时间系统, 提出了一种能够同时处理运行时间区间迭代变化以及未知时变时滞的预测迭代学习控制方法, 并通过理论分析给出了所提方法的收敛性质. 为处理运行时间区间迭代变化引起的数据丢失问题, 设计了一种新型的数据补偿机制, 利用历史数据信息和历史运行对未来的预报信息对缺失的数据进行有效补偿, 保证控制算法的有效更新. 为了克服未知时滞对系统产生

的影响, 将时滞的上下界信息引入控制算法中对其进行补偿. 通过仿真比较进一步验证了本文所提方法的有效性. 在未来的工作中, 将进一步提高所提方法对存在不确定性运行环境, 如执行器故障、外部干扰的适应能力.

参考文献:

[1] ARIMOTO S, KAWAMURA S, MIYAZAKI F. Bettering operation of robots by learning. *Journal of Robotic Systems*, 1984, 1(2): 123 – 140.

[2] YU Q, HOU Z. Adaptive fuzzy iterative learning control for high-speed trains with both randomly varying operation lengths and system constraints. *IEEE Transactions on Fuzzy Systems*, 2021, 29(8): 2408 – 2418.

[3] CHEN Y, HUANG D, LI Y, et al. A novel iterative learning approach for tracking control of high-speed trains subject to unknown time-varying delay. *IEEE Transactions on Automation Science and Engineering*, 2022, 19(1): 113 – 121.

[4] JI H, HOU Z, ZHANG R. Adaptive iterative learning control for high-speed trains with unknown speed delays and input saturations. *IEEE Transactions on Automation Science and Engineering*, 2016, 13(1): 260 – 273.

[5] SONG L, SHI J, ZHOU Y. Secant iterative learning control of ultrasonic motor. *ISA Transactions*, 2020, 103: 343 – 354.

[6] WANG Y, GAO Y, ZHAO C, et al. Iterative learning based torque ripple suppression of flux-modulation double-stator machine. *IEEE Transactions on Industrial Electronics*, 2022, 69(7): 6645 – 6656.

[7] YANG L, LI Y, HUANG D, et al. Spatial iterative learning control for robotic path learning. *IEEE Transactions on Cybernetics*, 2022, 52(7): 5789 – 5798.

[8] OH D, BAEK S, NAM K, et al. Tracking and synchronization with inversion-based ilc for a multi-actuator-driven wafer inspection cartridge transport robot system. *Electronics*, 2021, 10(23): 2904.

[9] TAYEBI A. Adaptive iterative learning control for robot manipulators. *Automatica*, 2004, 40(7): 1195 – 1203.

[10] GLÜCK T, BLANK M, BÜCHL D, et al. Convex constrained iterative learning control using projection: Application to a smart power switch. *IEEE Transactions on Control Systems Technology*, 2018, 26(5): 1818 – 1825.

[11] XI Yugeng, LI Dewei, LIN Shu. Model predictive control-status and challenges. *Journal of Automatica Sinica*, 2013, 39(3): 222 – 236.
(席裕庚, 李德伟, 林姝. 模型预测控制–现状与挑战. 自动化学报, 2013, 39(3): 222 – 236.)

[12] HONG Yingdong, XIONG Zhihua, JIANG Yongheng, et al. Iterative learning control for point-to-point integrated prediction based on 2D theory. *Control and Decision*, 2018, 33(3): 431 – 438.
(洪英东, 熊智华, 江永亨, 等. 基于2D理论的点对点综合预测迭代学习控制. 控制与决策, 2018, 33(3): 431 – 438.)

[13] SHI J, ZHOU H, CAO Z, et al. A design method for indirect iterative learning control based on two-dimensional generalized predictive control algorithm. *Journal of Process Control*, 2014, 24(10): 1527 – 1537.

[14] WANG L, SUN L, LUO W. Robust constrained iterative learning predictive fault-tolerant control of uncertain batch processes. *Science China Information Sciences*, 2019, 62(11): 219201.

[15] ZHANG R, GAO F. Two-dimensional iterative learning model predictive control for batch processes: A new state space model compensation approach. *IEEE Transactions on Systems, Man, and Cybernetics: Systems*, 2021, 51(2): 833 – 841.

[16] WANG L, FREEMAN C, CHAI S, et al. Predictive-repetitive control with constraints: From design to implementation. *Journal of Process Control*, 2013, 23(7): 956 – 967.

[17] CHU B, OWENS D, FREEMAN C. Iterative learning control with predictive trial information: convergence, robustness, and experimental verification. *IEEE Transactions on Control Systems Technology*, 2016, 24(3): 1101 – 1108.

[18] YAN Fei, LI Pu, XU Xinying. Traffic signal hybrid control method based on iterative learning and model predictive control. *Control Theory & Applications*, 2021, 38(3): 339 – 348.
(闫飞, 李浦, 续欣莹. 基于迭代学习与模型预测控制的交通信号混合控制方法. 控制理论与应用, 2021, 38(3): 339 – 348.)

[19] MA Lele, LIU Xiangjie. Robust model predictive iterative learning control with iteration-varying reference trajectory. *Journal of Automatica Sinica*, 2019, 45(10): 1933 – 1945.
(马乐乐, 刘向杰. 变参考轨迹下的鲁棒迭代学习模型预测控制. 自动化学报, 2019, 45(10): 1933 – 1945.)

[20] LU J, CAO Z, GAO F. Multipoint iterative learning model predictive Control. *IEEE Transactions on Industrial Electronics*, 2019, 66(8): 6230 – 6240.

[21] YU Q, HOU Z. Data-driven predictive iterative learning control for a class of multiple-input and multiple-output nonlinear systems. *Transactions of the Institute of Measurement and Control*, 2016, 38(3): 266 – 281.

[22] YU Q, HOU Z, BU X, et al. RBFNN-based data-driven predictive iterative learning control for nonaffine nonlinear systems. *IEEE Transactions on Neural Networks and Learning Systems*, 2020, 31(4): 1170 – 1182.

[23] WANG Jing, ZHOU Nan, WANG Sen, et al. Feedback-assisted PD-type quantized iterative learning control with randomly iteration varying lengths. *Control and Decision*, 2021, 36(10): 2569 – 2576.
(王晶, 周楠, 王森, 等. 随机变批次长度的反馈辅助PD型量化迭代学习控制. 控制与决策, 2021, 36(10): 2569 – 2576.)

[24] BU X, WANG S, HOU Z, et al. Model free adaptive iterative learning control for a class of nonlinear systems with randomly varying iteration lengths. *Journal of the Franklin Institute*, 2019, 356(5): 2491 – 2504.

[25] SHI J, XU J, SUN J, et al. Iterative learning control for time-varying systems subject to variable pass lengths: Application to robot manipulators. *IEEE Transactions on Industrial Electronics*, 2020, 67(10): 8629 – 8637.

[26] SHEN D, ZHANG W, XU J. Iterative learning control for discrete nonlinear systems with randomly iteration varying lengths. *Systems and Control Letters*, 2016, 96: 81 – 87.

[27] WEI Y, LI X. Robust higher-order ILC for non-linear discrete-time systems with varying trail lengths and random initial state shifts. *IET Control Theory & Applications*, 2017, 11(15): 2440 – 2447.

[28] LIU Q, ZHOU B. Delay compensation of discrete-time linear systems by nested prediction. *IET Control Theory & Applications*, 2016, 10(15): 1824 – 1834.

[29] BRESCH-PIETRI D, MAZENC F, PETIT N. Robust compensation of a chattering time-varying input delay with jumps. *Automatica*, 2018, 92: 225 – 234.

[30] WANG H, LIU S, YANG X. Adaptive neural control for non-strict-feedback nonlinear systems with input delay. *Information Sciences*, 2020, 514: 605 – 616.

[31] LÉCHAPPÉ V, DE L E, MOULAY E, et al. Delay and state observation for SISO nonlinear systems with input delay. *International Journal of Robust and Nonlinear Control*, 2018, 28(6): 2356 – 2368.

[32] HOU Z, XIONG S. On model-free adaptive control and its stability analysis. *IEEE Transactions on Automatic Control*, 2019, 64(11): 4555 – 4569.

[33] HOU Z, CHI R, GAO H. An overview of dynamic-linearization-based data-driven control and applications. *IEEE Transactions on Industrial Electronics*, 2017, 64(5): 4076 – 4090.

[34] XIONG S, HOU Z. Model-free adaptive control for unknown MIMO nonaffine nonlinear discrete-time systems with experimental validation. *IEEE Transactions on Neural Networks and Learning Systems*, 2022, 33(4): 1727 – 1739.

[35] ZHU P, JIN S, BU X, et al. Improved model-free adaptive control for mimo nonlinear systems with event-triggered transmission scheme and quantization. *IEEE Transactions on Cybernetics*, 2022: DOI: 10.1109/TCYB.2022.3203036.

[36] HOU Z, JIN S. Data-driven model-free adaptive control for a class of MIMO nonlinear discrete-time systems. *IEEE Transactions on Neural Networks*, 2011, 22(12): 2173 – 2188.

[37] GOODWIN G C, SIN K S. *Adaptive Filtering Prediction and Control*. Massachusetts: Courier Corporation, 2014.

[38] LI X, SHEN D, DING B. Iterative learning control for output tracking of nonlinear systems with unavailable state information. *IEEE Transactions on Neural Networks and Learning Systems*, 2022, 33(9): 5085 – 5092.

[39] LI Z, YANG G. Data-driven adaptive fault-tolerant control for a class of multiple-input-multiple-output linear discrete-time systems. *IET Control Theory & Applications*, 2017, 11(16): 2824 – 2833.

[40] XU D, JIANG B, SHI P. A novel model-free adaptive control design for multivariable industrial processes. *IEEE Transactions on Industrial Electronics*, 2014, 61(11): 6391 – 6398.

[41] ESMAEILI B, SALIM M, BARADARANNIA M. Predefined performance-based model-free adaptive fractional-order fast terminal sliding-mode control of MIMO nonlinear systems. *ISA Transactions*, 2022, 13(1): 108 – 123.

[42] LIANG J, BU X, CUI L, et al. Data-driven bipartite formation for a class of nonlinear mimo multiagent systems. *IEEE Transactions on Neural Networks and Learning Systems*, 2021: DOI: 10.1109/TNNLS.2021.3111893.

[43] Hou Zhongsheng, Jin Shangtai. *Model Free Adaptive Control*. Beijing: Science Press, 2013.
(侯忠生, 金尚泰. 无模型自适应控制. 北京: 科学出版社, 2013.)

[44] LEE T, TAN K, LIM S, et al. Iterative learning control of permanent magnet linear motor with relay automatic tuning. *Mechatronics*, 2000, 10(1/2): 169 – 190.

作者简介:

余琼霞　副教授, 硕士生导师, 目前研究方向为数据驱动控制、无模型自适应控制、学习控制等, E-mail: qiongxiayu@hotmail.com;

田丰臣　硕士研究生, 目前研究方向为非线性系统控制、学习控制等, E-mail: 212007010037@home.hpu.edu.cn;

孙俊杰　工程师, 目前研究方向为矿用运输车辆自动运行控制、无人机建模、矿区铁路无人道口自动化防护等, E-mail: 116719406@qq.com;

侯忠生　教授, 博士生导师, 目前研究方向为数据驱动控制、无模型自适应控制、学习控制、智能交通等, E-mail: zhshhou@bjtu.edu.cn.